M-AM-J7

PHOTORECEPTOR-TRANSDUCER MOLECULAR COMPLEX OF SENSORY-RHODOPSIN-I: A ROTATIONAL DIFFUSION STUDY.
((R. A. **Bogomolni**, J.G Fukushima, T. Swartz and I. Szundi)) Department of Chemistry and Biochemistry, University of California, Santa Cruz.

We used photoselection spectroscopy to probe the rotational motions of native sensory rhodopsin-I (sR-I) and of sR-I free of its transducer HtrI (tsR-I). We measured transient polarization anisotropy changes during the photocycles of sR-I and tsR-I in cell membrane pellets of wild-type and HtrI-deficient Halobacterium salinarum strains respectively, in which sR-I is the only photochemically-active pigment. As reported earlier (Biophys. J. 57 :539 (1990)) sR-I shows a flash-induced anisotropy decaying with half-times in the 30-300 microsecond range from initial values around 0.34 (theoretical maximum = 0.4) to non-zero limiting values around 0.1. In contrast tsR-I shows a rapidly decaying anisotropy ($t_{1/2}$< 30 microsec.) to a non-zero limiting value around 0.04-0.06. Analysis of the data in terms of restricted molecular motions around an axis perpendicular to the membrane plane are consistent with a model in which the rapidly-rotating tsR-I is perhaps a monomer or a small oligomer (the uncertainty originates mainly from our lack of knowledge of the local membrane viscosity). From the limiting anisotropy we calculate that the angle of its retinal chromophore with respect to the membrane plane is around 20°. Native sR-I, in contrast, shows significantly hindered motion as expected if it is bound to its transducer, as well as a different chromophore angle. Assuming similar membrane viscosity in the two strains, the long anisotropy decay times for native sR-I **cannot** be accounted for by a model in which sR-I and HtrI exist in a 1:1 ratio in the complex. Higer stoichimetries and/or interaction with other membrane or cytoplasmic proteins may be invoked.

M-AM-J8

RELAXATION DYNAMICS OF THE TWISTED CHROMOPHORE OF THE PRIMARY PHOTOPRODUCTS OF BACTERIORHODOPSIN AND HALORHODOPSIN. ((A. K. Dioumaev and **M. S. Braiman**)) Biochemistry Department, University of Virginia Health Sciences Center, Charlottesville, VA 22908.

We have analyzed the red-shifted photoproducts of bacteriorhodopsin (bR) and halorhodopsin (hR) on the ns time scale using step-scan Fourier transform infrared spectroscopy. Both the primary K photoproduct of bR and the corresponding hK photoproduct of hR are known to have significant twists in their retinylidene protonated Schiff base chromophores. We have characterized previously-unobserved relaxations in these twisted chromophore conformations occurring with time constants of $\tau_K \simeq$50–100 ns for K and $\tau_{hK} \simeq$250 ns for hK (measured at 20°C). These transitions are clearly distinguishable in the time-resolved IR spectral measurements from much-slower transitions to the L and hL photoproducts. We designate the earlier and later forms of the bR bathophotoproducts as K_E and K_L, and the corresponding hR photoproducts as hK_E and hK_L. The transitions between these 2 forms of K, and between the corresponding 2 forms of hK, have never been observed in visible spectroscopic measurements on the sub-μs time scale. Nevertheless, both the $K_E \rightarrow K_L$ and $hK_E \rightarrow hK_L$ transitions are characterized by substantial intensity decreases and frequency shifts of several vibrations of the chromophore's Schiff base, including the C=N stretch and the C_{15}-H out-of-plane wag.
Supported by NIH grant GM46854 and Fogarty Fellowship TW05212.

M-AM-J9

CRYSTALLOGRAPHIC STUDIES OF THE FIRST INTERMEDIATE IN THE PHOTOCYCLE OF THE BIOLOGICAL LIGHT SENSOR PHOTOACTIVE YELLOW PROTEIN (PYP).
Ulrich K. Genick, Ilona Canestrelli, Elizabeth D. Getzoff, Department of Molecular Biology, The Scripps Research Institute, La Jolla, California 92037, USA

The cis-trans isomerizations during the formation of the first intermediate in light cycles of many biological photoreceptors are among the fastest reactions in biology. Yet they take place in the densely packed interior of proteins. How is it possible to perform such fast reactions in a spatially restrained environment and still generate a chromophore geometry that is able to trigger the large scale structural rearrangements that occur in the later stages of protein photocycles? To answer these questions we use low temperature trapping combined with cryo-crystallography and ultrafast time-resolved Laue crystallography to determine the structure of the first intermediate in the light cycle of Photoactive Yellow Protein. PYP is a cytosolic photoreceptor from Ectothiorhodospira halophila that has proven unusually amenable to structural studies. We have previously determined the structure of PYP's ground state (Borgstahl et al.1995 *Biochemistry* 34, 6278-6287) and of the late intermediate (Genick et al. *Science* accepted). Difference electron density maps generated from our cryo-crystallographic experiments indicate that the changes during the formation of the early intermediate are restricted to the chromophore and indicate only minimal movement in PYP's *p*-hydroxycinnamyl chromophore.

SOCIETY AWARD WINNERS SYMPOSIUM

Awards-Sym-1 *1997 Young Investigator Award Winner*
D. W. Hilgemann, University of Texas SW Medical Center
Regulation of Ion Channels and Transporters by Inositol-Containing Phospholipids

Awards-Sym-2 *1996 Margaret Oakley Dayhoff Award Winner*
S. Marqusee, University of California, Berkeley
Dissection of the Protein Folding Problem: Studies of Partially Folded Proteins

Awards-Sym-3 *1997 Winner of the Avanti Award in Lipids*
C-h. Huang, University of Virginia
A Combined Calorimetric/Molecular Mechanics Investigation of Bilayers Composed of Saturated and/or Unsaturated Mixed-chain PC or PE

Awards-Sym-4 *1997 Elisabeth Roberts Cole Award Winner*
W. H. Woodruff, Los Alamos National Laboratory
Time-Resolved Vibrational Studies of the Fast Events in Protein Folding

Awards-Sym-5 *1997 Distinguished Service Award Winner*
T. D. Pollard, Salk Institute
Scientists as Political Advocates

M-PM-SymI-1 **J. Fox, Axon Instruments, Inc.**
Channel Block Shapes Current and Reveals Structure of Channels

M-PM-SymI-2 **J. Lansman, University of California, San Francisco**
Neuronal Calcium Channel Gating by a Cytoplasmic Blocking Particle

M-PM-SymI-3 **A. Picones, University of California, San Francisco**
Permeation and Blockage of Photoreceptor cGMP-gated Ion Channels by Divalent Cations

M-PM-SymI-4 **G. Yellen, Harvard University**
What Blockade can Tell Us About Gating Motions of Voltage-gated Potassium Channels

M-PM-SymI-5 **L. Nowak, Cornell University**
Voltage-dependence of the Mg^{2+} Block of NMDA Channels Revisited

SWITCHES AND MOTORS: COMMON FEATURES OF G PROTEINS, KINESIN AND MYOSIN

M-PM-SymII-1 **H. E. Hamm, Northwestern University Medical School**
The GTP-dependent Conformational Switch in Heterotrimeric G Proteins: Role in Controlling Signaling Machinery

M-PM-SymII-2 **R. D. Vale, HHMI, University of California, San Francisco**
Molecular Motors and G Proteins: Common Structural and Mechanistic Themes

M-PM-SymII-3 **A. M. Gulick, University of Wisconsin**
Domain Movements and Switches in the Catalytic Mechanisms of Myosin

M-PM-SymII-4 **H. L. Sweeney, University of Pennsylvania**
The Switch Elements in Myosin: Structures, Mutations and Speculation

ACTOMYOSIN INTERACTION

M-PM-A1

KINETIC CHARACTERIZATION OF MYOSIN MUTATIONS THAT CAUSE FAMILIAL HYPERTROPHIC CARDIOMYOPATHY.
((**Osha Roopnarine** and Leslie A. Leinwand)) Dept of Molecular, Cellular, and Developmental Biol. Univ. of Colorado, Boulder, CO.

We are studying the functional properties of myosin mutants that cause **familial hypertrophic cardiomyopathy** (FHC). To determine the effect of the mutations on myosin ATPase activity, we have co-expressed histidine-tagged rat cardiac myosin subfragment-1 (S1) along with rat ventricular light chain 1 (VLC1) in mammalian cells (COS). The S1s studied were wildtype α and β and three FHC mutations (Arg249Gln, Arg403Gln, and Val606Met). The crystal structure of S1 indicates that these mutations are near the ATP-binding (249-S1) and actin-binding (403-S1 and 606-S1) regions. The S1s and associated VLC1 were purified from the cell lysate by an affinity resin (nickel-agarose) that binds to the His-tag at the C-terminal of the S1. We have previously established that α- and β-S1 expressed and purified from COS cells retain physiological ATPase properties (Roopnarine and Leinwand, 1996, *Biophys. J*, A172). Our present results show that the actin-activated ATPases of the purified S1s are: α-S1 $\approx$ 606-S1 > β-S1 > 403-S1 > 249-S1, indicating that two of the mutations affect the activation of myosin ATPase by actin.

M-PM-A2

BIOCHEMICAL AND KINETIC CHARACTERIZATION OF MUTANT MYOSIN MOTOR DOMAINS WITH GREATLY SLOWED ATP HYDROLYSIS STEPS
((**A.L. Friedman**[1], H.M. Warrick[1], A. Spudich[1], D.J. Manstein[2], M.A. Geeves[3], & J.A. Spudich[1])) [1]Biochemistry Department, Stanford University, Palo Alto, CA, 94305, [2]Max-Planck-Institute for Medical Research, 69120 Heidelberg, Germany, and [3]Max-Planck-Institute for Molecular Physiology, 44026 Dortmund, Germany

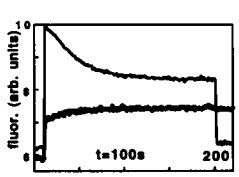

Tens of milligrams of a minimal motor, M761-1R, consisting of the *Dictyostelium discoideum* catalytic domain and one α-actinin repeat inserted in place of the native light chain binding domain, are being expressed and purified using a C-terminal His tag (Manstein & Hunt, 1995, J. Muscle Res. Cell Motil. 16:325-332). The kinetics and actin-motility properties of these fusion proteins are closely similar to *Dictyostelium* S-1 (Anson, Geeves, Kurzawa, & Manstein, EMBO, in press). When 2'(3')-O-(N-Methylanthraniloyl)-ATP (mantATP) binds stoichiometrically to M761-1R (t=10s, upper/thinner trace in Fig.) the fluorescence increases rapidly and then decreases with a rate consistent with the rate of Pi release (t=10-200s). The evolved mantADP can be chased with excess ATP (t=200s). Two point mutations inserted into M761-1R, E459V (lower/thicker trace) or E476K (Ruppel & Spudich, 1996, Molec. Biol. Cell 7:1123-1136), result in an at least an order of magnitude reduction of the ATP hydrolysis step of the ATPase cycle (note lack of decay from t=10-200s); the bound fluorescent nucleotide is chased to a small (E476K) or very small (E459V, see Fig.) extent after 200 s. The estimated ATP turnover period of E476K is ~30 min.

M-PM-A3

Cross-bridges are in Weak-Binding States in the Presence of High Concentrations of AMP-PNP in Skinned Rabbit Psoas Muscle. ((S.M. Frisbie*, J. M. Chalovich+, L.C. Yu*)). *NIH, Bethesda, MD;+East Carolina University, School of Medicine, NC.

AMP-PNP was thought to produce strong binding crossbridge states that can activate the regulatory system. In the present study, the equatorial intensity ratio I_{11}/I_{10} is shown to decrease with increasing AMP-PNP concentration. This indicates increasing detachment of crossbridges. At 1°C and 170 mM ionic strength, the I_{11}/I_{10} ratio decreased until it plateaued at approx. 20 mM AMP-PNP in EGTA-containing solution, suggesting full saturation with the nucleotide. Under saturating conditions, crossbridges were found to be weak-binding: 1) The affinity of S1-AMP-PNP for actin-troponin-tropomyosin is weak ($4 \times 10^3 M^{-1}$), 2) The two dimensional X-ray diffraction pattern (equatorial intensities and myosin layer lines) for AMP-PNP relaxed muscle is indistinguishable from the ATP-relaxed pattern in EGTA, 3) I_{11}/I_{10} is sensitive to ionic strength as seen for weak-binding crossbridges in the presence of ATP. AMP-PNP saturation was dependent on ionic strength and temperature. Furthermore, in CaEGTA-containing solution a plateau was never reached even at 40 mM nucleotide, supporting our earlier findings that crossbridge affinity for nucleotides is Ca^{++}-dependent in muscle fibers.

M-PM-A4

ESSENTIAL LIGHT CHAIN-1 MODULATES THE ACTOMYOSIN INTERACTION IN THE ABSENCE OF THE N-TERMINAL ACTIN BINDING SITE. ((**Lakshmi D. Saraswat**, Megan King and Susan Lowey)) Rosenstiel Research Center, Brandeis University, Waltham, MA 02254.

The diversity of myosin heavy chain and light chain isoforms is responsible for many of the contractile properties of striated muscles. Adult fast muscles contain two ELC isoforms, LC1 and LC3, which differ primarily in an additional 41 residues rich in Pro, Ala, Lys at the N-terminus of LC1. The unloaded shortening velocity of single fibers has been shown to be proportional to the relative ratio of LC1 to LC3. An estimate of the length of the N-terminus was obtained by engineering two cysteines spanning ~40 residues in LC1. Fluorescence energy transfer gave an average distance of 44±4 Å between Cys pairs modified with IAEDANS as the donor, and DDPM (R_o=30Å), DABM (R_o=40Å) or IAF (R_o=50Å) as the acceptor. A deletion mutant (truncated LC1) missing the first 14 residues, thought to contain an actin binding site, was exchanged into myosin and its actin filament sliding velocity was compared to myosin containing intact LC1. Both reconstituted myosins moved actin more slowly in a motility assay (~5 μm/s) than myosin containing the LC3 isoform (~7 μm/s). In an actin assembly assay, S1 containing LC1 or truncated LC1 polymerized G-actin more rapidly than S1(LC3). Even though the N-terminus of LC1 may be sufficiently elongated to interact directly with actin, as proposed earlier, sequences inherent in the truncated LC1 may also modulate the functional properties of myosin.

M-PM-A5

MYOSIN REGULATORY LIGHT CHAIN AND NUCLEOTIDE MODULATION OF ACTIN BINDING SITE ELECTRIC CHARGE ((**S. Highsmith**)) Department of Biochemistry, UoP, San Francisco, CA 94115-2399

The ionic strength dependence of skeletal muscle myosin subfragment 1 (S1) binding to actin in the presence of ADP and ATP was measured for S1 with either only an essential light chain (S1(elc)) or with both an essential and the regulatory light chain (S1(elc,rlc)) bound. The data were analyzed to determine the apparent association constant, K_A, for actin binding, and the absolute value of the product of the net effective electric charges at the actin-myosin interface, $|z_M z_A|$. When MgADP is bound at the myosin active site, K_A values at 0 M ionic strength for S1(elc) and S1(elc,rlc) are 12 and 4.9×10^6 M^{-1}, respectively, and $|z_M z_A|$ is 3.5 ± 1 esu^2 for both species. In the presence of ATP, K_A values at 0 M ionic strength for S1(elc) and S1(elc,rlc) are 81 and 7.3×10^4 M^{-1}, respectively, and $|z_M z_A|$ values are 14.5 esu^2 for S1(elc), but only 6.3 esu^2 for S1(elc,rlc). These results indicate that the regulatory light chain can regulate the interactions of myosin and actin by modulating the electric charge at the actin binding site. Measurements were also made at 25°C for S1(elc,rlc) binding to actin in the presence of the ATP analog, ATPγS. At 0 M ionic strength, K_A is 8.0×10^4 M^{-1}, and $|z_M z_A|$ is 0, within experimental uncertainty, suggesting that for S1.MgATP the electric charge at the actin binding site is abolished. The results suggest that crossbridge dissociation by ATP requires abolition of charge and that the large increase in electric charge for S1.MgADP.P_i is used to guide the crossbridge electrostatically to a new actin.

M-PM-A6

PROBING THE INTERACTION OF LYS-553 OF MYOSIN WITH ACTIN BY FLUORESCENCE SPECTROSCOPY. ((**Christopher L. Berger**)). Dept. of Molecular Physiology & Biophysics, Univ. of Vermont, Burlington, VT 05405.

It has been suggested that the helix-loop-helix motif in the lower half of the 50 kD subdomain of myosin containing Lys-553 forms a stereospecific interaction with actin (Rayment et al., *Science* 261:58-65). Bertrand et al. (1995, *Biochemistry* 34:9500-9507) observed that Lys-553 could be specifically and extensively modified with the fluorescent probe FHS (6-[fluorescein-5(and 6)-carboxamidohexanoic acid succinimidyl ester) in S1, but that this reaction is blocked by actin. To further clarify the interaction between myosin at Lys-553 and actin, we have examined the effects of solvent quenching on the fluorescence from S1 labeled with FHS at Lys-553 (FHS-S1). Three different solvent quenchers varying in charge were used; negatively charged iodide ions, positively charged thallium ions, and a neutral nitoxide, TEMPO. In the absence of actin, all three quenchers effectively quench the FHS fluorescence. It was expected that, if Lys-553 is indeed at the actin-binding interface, the binding FHS-S1 to actin in a rigor complex would protect the fluorescein probe from solvent quenching. However, binding to actin offered no protection from solvent quenching by either thallium or TEMPO, but did reduce the Stern-Volmer constant for iodide quenching by almost two-fold. Thus, it is likely that Lys-553 is situated near a negatively charged side chain on actin when FHS-S1 binds in a rigor complex, or that the solvent access to Lys-553 is restricted by actin such that the fluorescein probe is only exposed near a negative charge on myosin.

M-PM-A7

PROBING CONFORMATIONAL CHANGES IN MYOSIN DURING THE ATPase CYCLE. ((**Wenchuan Liang**, William Shih & James A. Spudich)), Department of Bichemistry, Stanford University, Stanford, CA 94305-5307

Myosins hydrolyze ATP and use the derived chemical energy to produce force and directed movement along actin filaments. It has been proposed that the state of the 50 kDa cleft provides a mechanism for communication between the spatially distinct actin and ATP binding sites which in turn paces the timing and duration of power stroke (1). The molecular basis of the mechanism is not known. We are applying chemical thiol-crosslinking techniques to probe these conformational changes.

The reactive thiols (SH1 and SH2) are in the fulcrum region that is thought to undergo a large conformational change upon binding ATP. In skeletal muscle with nucleotides, SH1 and SH2 move from further than 14 Å apart to as close as 3 Å, based on studies using thiol cross-linking reagents with varying length (2). Like many non-muscle myosins, *Dictyostelium* myosin lacks a cysteine corresponding to SH1. We have created a plasmid containing a "cyslite" myosin gene in which nearly all the cysteines are removed. We have also engineered both SH1 and SH2 in the cyslite myosin gene, and shown that this gene is able to rescue the null cells *in vivo*. Currently, chemical crosslinking reactions and *in vitro* characterization are undergoing.

(1) Fisher, A.J., Smith, C.A., Thoden, J., Smith, R., Sutoh, K. et al. (1995) Structural Studies of myosin:nucleotide complexes: a revised model for the molecular basis of contraction. **Biophys. J. 68**: 19s-28s.

(2) Wells, J.A. & Yount, R.G. (1979) Active site trapping of nucleotides by crosslinking two sulfhydryls in myosin subfragment 1. **Proc. Natl. Acad. Sci. U.S.A.** 76:4966-4970.

M-PM-A8

FRET MEASUREMENTS OF DISTANCES BETWEEN CYS-177 ON LIGHT CHAIN A1 AND THREE POINTS ON THE HEAVY CHAIN OF SKELETAL S1 UPON FORMATION OF COMPLEXES WITH MG·ADP·BeF_3, MG·ADP·AlF_4, AND MG·ADP·V_i ((CYBELLE SMYCZYNSKI AND **Andrzej A. Kasprzak**)) *CRBM du CNRS, Route de Mende, 34033 Montpellier, France*

Several lines of evidence suggest that in order to produce a ~10 nm step, myosin may use its light-chain-binding domain as a lever to amplify small changes in the catalytic domain. To probe the spatial position of the LC-binding helix, we measured distances from Cys-177 of LC A1 to three points of the S1 heavy chain: Lys-83, the active site and Ser-180, by resonance energy transfer (FRET). The measurements were performed for S1 alone, its complexes with MgADP and MgATP, and for the analogues of the transition state of the ATPase reaction: S1·ADP·BeF_3, S1·ADP·$AlCl_4$, and S1·ADP·V_i. Cys-177 of LC A1 was labeled with 1,5-IAEDANS or 5-iodoacetamidofluorescein, Lys-83 was labeled with 2,4,6-trinitrobenzenesulfonate, TNP-ADP at the active site was used as an analog of ADP; fluorescent modification of Ser-180 was performed with 9-anthroylnitrile in the presence of ATP. The modified S1 derivatives were capable of forming complexes with BeF_3, AlF_4, or V_i. The distances found in the absence of the analogues were in general agreement with the values obtained by X-ray or previous FRET studies. When the transition state complexes were formed only small alterations of the measured distances were observed, although changes in position of Cys-177 would be easily detected by FRET if the light chain binding domain rotated by about 20° (or more) as seen recently for smooth muscle S1. In one case, the distance Cys-177→TNP·ADP changed significantly in the presence of AlF_4^-. Several possible explanations of these findings are offered.

M-PM-B1

NMR-BASED STRUCTURE-FUNCTION RELATION OF N-TYPE INACTIVATION IN K_V-TYPE K^+ CHANNELS

((Ch. Antz, J.P. Ruppersberg and B. Fakler)) Department of Physiology II, University of Tuebingen, Gmelinstr. 5, 72076 Tuebingen, Germany

Rapid inactivation of voltage-gated K^+ (K_V) channels is mediated by an N-terminal domain (inactivation gate or inactivation ball) which blocks the open channel from the cytoplasmic side. Even when synthesized as a peptide, such ball domains can fully restore inactivation in K_V channels which lack inactivation balls or whose inactivation domains have been deleted. Using high-resolution NMR-spectroscopy we have analyzed the three-dimensional structure of the ball peptides of Raw3 (K_V3.4) and RCK4 (K_V1.4), two mammalian K_V channels. In aequous solution both inactivation peptides (IP) were found to exhibit a well-defined structure exposing the sites of oxidation (Raw3-IP and RCK4-IP) and phosphorylation (Raw3-IP) at the molecular surface. Although their backbone structure is rather different, both IPs showed a similar spatial distribution of charged and hydrophobic surface domains. These NMR-derived stuctures were now correlated with functional properties using fast application of synthetic peptides on non-inactivating K_V 1.1 (RBK1) channels. Mutations destroying the overall structure of the IPs lead to a complete loss of their ability to close open channels with low voltage-dependence. Mutations that altered the structure of both wild-type IPs allowed identification of structural domains responsible for blocking and unblocking in both IPs.

M-PM-B2

A MOLECULAR TOPOLOGY OF THE EXTERNAL VESTIBULE OF A K CHANNEL. ((D. Naranjo and C. Miller)) HHMI, Dept. of Biochemistry, Brandeis University, Waltham, MA 02254.

α-K-toxins like charybdotoxin (CTX) make up a family of peptides of known molecular structure that bind with high specificity to the external mouth opening of K-channels and thus block current. Each toxin member becomes a distinct molecular caliper to probe the K channel architecture. A critical conserved residue, Lys-27, plugs the pore and defines the axis of symmetry of the channel-toxin interaction surface. We have made use of the specific interaction between CTX and the Shaker K channel, along with double-mutant cycle analysis (Hidalgo and MacKinnon, 1995, *Science* **268**:307) to probe those residues located on the N-terminal flank of the pore-forming loop. Recombinant toxins were expressed as a cleavable fragments of a fusion protein and recombinant Shaker K channels were expressed in *Xenopus* oocytes. Only channel mutants that expressed as homotetramers were studied. Dissociation constants for recombinant Shaker K channels and toxins were determined from current inhibition in two-electrode voltage-clamp. We found a consistent pattern of overlapped interacting pairs; toxin mutants at position 8 or 9 (12-15 Å above and 12-15 Å lateral to the ε-carbon of Lys-27) show interaction with mutants at 425 and 427 on the channel. Toxin mutants at position 31 (5-10 Å above and 12-15 Å lateral to Lys-27) show electrostatic interaction with channel residues at position 427 and 431. Residues 434 and 449 appear to be very close in space because they interact with identical residues in close proximity to Lys-27 (25, 36, and 29). This pattern of contacts is consistent with an α-helical conformation for the N-terminal flank of the P-region 15-25° tilted with respect to the plane of the membrane. Partially supported by GM-31768.

M-PM-B3

USE OF HYDROPHILIC AMINO ACID EPITOPE INSERTIONS TO PROBE THE TOPOLOGY OF THE *SHAKER* H4 POTASSIUM CHANNEL. ((T.M. Shih and A.L. Goldin)) Department of Microbiology and Molecular Genetics, University of California, Irvine, CA 92697.

The structure of the *Shaker* H4 potassium channel has been modeled as passing through the cellular membrane eight times, with both the N- and C-termini on the cytoplasmic side (Durell and Guy, 1992, Biophys.J., 62:238-250). To test the validity of this structural model, we have inserted an epitope consisting of eight hydrophilic amino acids (DYKDDDDK, termed FLAG) in regions throughout the channel. The channels containing the synthetic epitope were expressed in *Xenopus* oocytes, and function was examined by two electrode voltage-clamping. Directed immunofluorescent staining was used to determine the membrane location of the epitope in each of the insertion mutants. Extracellular epitopes were identified by incubating intact oocytes with the M2 anti-FLAG antibody before fixation and fluorescent labeling. Intracellular epitopes were identified by injecting the M2 antibody into intact oocytes before fixation and fluorescent labeling. The boundaries of the exposed regions were determined by placing epitopes close to the membrane barrier. Localization of epitope insertions in the N-terminus, S1-S2 loop, S3-S4 loop, S5-pore region, and C-terminus have proved to be consistent with the Durell and Guy model. Data concerning the electrophysiology and localization of these insertions will be presented.

M-PM-B4

ACTIVATION OF A WEAKLY VOLTAGE DEPENDENT K^+-CURRENT BY THE NEUROPEPTIDE FMRFa IN IDENTIFIED MOLLUSCAN NEURONS

((Karel S. Kits and M.J. Veerman)) Membrane Physiology Section
Research Institute Neurosciences, Vrije Universiteit, De Boelelaan 1087,
1081 HV Amsterdam, The Netherlands
Telephone: +31-20-4447096, Telefax: +31-20-4447123, E-mail: ksk@bio.vu.nl

The neuropeptide Phe-Met-Arg-Phe-amide (FMRFa) acts as an inhibitory neurotransmitter in the molluscan cns. In the peptidergic Caudodorsal Neurones that regulate egg laying in the snail *Lymnaea stagnalis*, FMRFa dose dependently (ED_{50}~ $2*10^{-8}$ M) activates a K^+-current. Under standard conditions ($[K^+]_o$= 1.7 mM, $[K^+]_i$= 57 mM) FMRFa evoked only outward current responses. With $[K^+]_o$ increased to 20 or 57 mM K^+, the current reversed close to the theoretical reversal potential for K^+. The IV relations in high K^+ salines revealed that at voltages below -60 mV, the current amplitude decreased while the driving force increased. In both salines no responses were measured at potentials below -120 mV. These results imply that the K^+ channels involved in this response are voltage-dependent. Furthermore, comparison of activation curves (plots of conductance versus voltage) for different $[K^+]_o$, showed that the conductance increased with increasing extracellular K^+ concentrations.

The response to FMRFa was affected when the cells were dialyzed with GTPγS, indicating that the FMRFa-receptor is coupled to a G-protein. The response was further inhibited by blockers of phospholipase A_2 and lipoxygenases, but not by a blocker of cyclo-oxygenase (indomethacine). Bath application of arachidonic acid resulted in a slow outward current, while in the presence of arachidonic acid the response to the FMRFa was decreased. These results suggest that the FMRFa-receptor couples to arachidonic acid metabolism and employs lipoxygenase products in the intracellular signalling process.

M-PM-B5

DEVELOPMENTAL CHANGES IN THE EFFECTS OF QUINIDINE ON HUMAN ATRIAL TRANSIENT OUTWARD K^+ CURRENT (I_{to}). (N.I. Nenov,+ W.J. Crumb Jr.,* J.D. Pigott,# L.H. Harrison Jr.,* C.W. Clarkson*) Depts. Of Pharmacology,+ Pediatrics*, and Surgery,# Tulane Medical School, New Orleans, LA, and Dept. of Surgery,* LSU-Medical Center, New Orleans, LA

Clinical studies have demonstrated differences in the antiarrhythmic effectiveness of quinidine(Q) in pediatric and adult patients, and age-related changes in the interaction of Q with cardiac ion channels have been documented in rabbit. Developmental changes in the electrophysiological properties of human atrial I_{to} are also known to exist. This work tested the hypothesis that developmental changes in I_{to} are associated with age-dependent changes in the ability of Q to block this current in human atrial cells. Using the whole-cell voltage clamp technique, I_{to} was recorded from the hearts of pediatric (0-2 years) and adult (>8 years) patients at 22°C. During single pulses from -40 to +60 mV, 3 μM Q produced a similar degree of tonic block in pediatric and adult I_{to} (39±6%, n=8 and 38±3%, n=11 respectively). In contrast, during repetitive pulsing from -40 to +60 mV (20 ms) at 0.5, 1 and 2 Hz, 3 μM Q produced use-dependent block of I_{to} that was greater in adults than in pediatric cells. For example, pulsing at 1 Hz resulted in use-dependent decrease of I_{to} measuring 18±6% (n=5) in pediatric and 34±3%(n=10) in adult cells. 3 μM Q also produced a hyperpolarizing shift in the I_{to} half-inactivation voltage that was independent of age (adult:6.0±1.8mV, n=8; pediatric:9.6±1.8mV, n=11). A marked developmental difference was also documented in both the amplitude and voltage dependence of the time constant (τ_{rec}) of Q unblocking of I_{to}. τ_{rec} increased with hyperpolarization from -40 to -80 mV in adult cells (from 1.6±0.2 s to 2.5±0.3s, n=11) ($P<0.05$), and decreased slightly over the same voltage range in pediatric cells (from 3.2±0.7 s to 2.4±0.3, n=5). These results indicate that there are significant developmental differences in the interaction of quinidine with I_{to} in pediatric vs. adult human atrial myocytes.

M-PM-B6

INHIBITION OF THE Ca^{2+} -ACTIVATED K CHANNEL OF MURINE ERYTHROLEUKEMIA CELLS BY THE ANTIFUNGAL IMIDAZOLE, CLOTRIMAZOLE, AND ITS MAJOR *IN VIVO* METABOLITE IS INDEPENDENT OF BLOCKADE OF CYTOCHROME P450(**D.H. Vandorpe**, C. Brugnara, & S.L. Alper.)). Molecular Medicine & Renal Units, Beth Israel Hospital, and Departments of Medicine, Cell Biology and Pathology, Harvard Medical School, Boston, MA 02115.

Clotrimazole (CLT), a member of the antifungal imidazole family of compounds, has been found to inhibit both calcium (Ca^{2+})-activated ^{86}Rb and potassium (K) fluxes of human red cells and to inhibit red cell binding of ^{1}-charybdotoxin (ChTX). We recently showed in whole-cell patch clamp experiments that submicromolar concentrations of CLT reversibly inhibited whole cell K_{Ca} currents in murine erythroleukemia (MEL) cells. We have now used single channel patch clamp to determine the single channel basis of the CLT inhibition in MEL cells by demonstrating the inhibition of a calcium-activated, ChTX-sensitive K channel by CLT in outside-out patches. The channel was also blocked by the des- imidazolyl metabolite of CLT, 2-chlorophenyl-bisphenyl-methanol (MET II), thus demonstrating that the imidazole ring, absolutely required for inhibition of cytochrome P450, is not required for the inhibitory action of CLT. Single K_{Ca} channels of the same conductance were also evident in inside-out patches of MEL cells. Block of K current by CLT was not restricted to MEL cells. These results demonstrate that direct inhibition of single K_{Ca} by CLT can be dissociated from inhibition of cytochrome P450 in MEL cells.

M-PM-B7

TAXOL, A STABILIZER OF MICROTUBULES, INCREASES GATING INSTABILITY OF CA^{2+}-ACTIVATED K^+ CHANNELS. ((**Aaron Kitzmiller** and Robert Rosenberg)) University of North Carolina, Chapel Hill, NC 27599. (Spon. by Q.-Y. Liu)

In experiments designed to test the interaction of the cytoskeleton or cytoskeleton-associated proteins with large conductance, Ca^{2+}-activated K^+ (BK) channels, rat brain membranes were prepared in the presence or absence of the cytoskeleton stabilizing drugs, taxol and phalloidin. In the presence of these drugs, single BK channels incorporated into planar bilayers exhibit wide fluctuations in steady state open probability (P_o) similar to the "Wanderlust" gating observed in Xenopus oocytes (Silberberg, et al. 1996 Biophys.J. 70:2640). The gating instability was much larger than that seen in channels from control preparations, and cannot be accounted for by the stochastic variation in simple, accepted Markov models. Taxol alone was able to reproduce this enhanced instability, consistent with the hypothesis that the fluctuations in P_o are a result of BK channel regulation by microtubules, one of the microtubule-associated proteins, or tubulin. As predicted by known interactions of cytoskeletal proteins with biological membranes, P_o fluctuations were strongly reduced by the omission of acidic phospholipids from the bilayer .

M-PM-B8

APAMIN-SENSITIVE K^+ CHANNELS IN SMOOTH MUSCLE ACTIVATED BY PURINOCEPTOR STIMULATION. ((**Fivos Vogalis** and Raj K. Goyal)) Harvard Medical School & Brockton/West Roxbury VAMC, 1400 VFW Parkway, West Roxbury MA 02132.

In smooth muscle,K^+ channels determine contractility by regulating voltage-dependent Ca^{2+} entry. Using amphotericin B-perforated patch whole-cell recording techniques on smooth muscle cells enzymatically dispersed from mouse ileum, we have identified a Ca^{2+}-dependent K^+ channel current which is sensitive to extracellular apamin (0.5 μM) (decreased from 88.6 ± 20 pA/pF to 21 ± 1.7 pA/pF, n=6 at $V_{t_{1/2}}$ 0 mV). In the whole-cell mode, an apamin-sensitive current was recorded at V_t positive of -60 mV when $[Ca^{2+}]_i$ was buffered to ~150 nM but was absent when $[Ca^{2+}]_i$ was reduced to < 85 nM. In cell-attached recordings, under an asymmetrical K^+ gradient (152 mM $[K^+]_{bath}$: 2.5 mM $[K^+]_{pipette}$) at a V_h of 0 mV unitary K^+ channel currents with conductances of 39 pS and >150 pS were active. In addition, a population of less clearly discernible ~10 pS channels was also present. In inside-out patches, all three channel types were sensitive to $[Ca^{2+}]_i$. Stimulation of P_{2y} receptors on the membrane outside the patch with 2-methylthioATP (2-MeSATP, 20-50μM) reversibly increased the open probability (NP_o) of the 39 pS K^+ channels at 0 mV from 0.16 ± 0.048 to 0.58 ± 0.11 (n=10) and activated an outward baseline current (0.76 ± 0.19 pA, n=8) but had little or no effect on the >150 pS channels. Inclusion of apamin (0.5 μM) in the pipette prevented the increase in NP_o of the 39 pS channels in response to 2-MeSATP and inhibited both the openings of the ~10 pS channels and activation of the outward baseline current (0.23 ± 0.06 pA, n=7). Inclusion of TEA (2 mM) in the pipette markedly inhibited the 39 pS channels but did not affect the activity of the ~10 pS channels. These small conductance channels increased their NP_o 4-fold from 0.073 ± 0.031 to 0.296 ± 0.121 (n=5) upon P_{2y} receptor stimulation in the presence of external TEA. Our findings confirm the presence of a class of intermediate conductance and a class of small conductance Ca^{2+}-dependent K^+ (SK_{Ca}) channels in smooth muscle that can regulate membrane potential at levels of $[Ca^{2+}]_i$ subthreshold for contraction and suggest that SK_{Ca} channels may mediate purinergic nerve mediated inhibition of smooth muscle contractility. (Supported by NIH grants DK50137 to F.V and DK31902 to R.J.K.)

PROTEIN FOLDING

M-PM-C1

ORIGIN OF ENTROPY CONVERGENCE IN PROTEIN FOLDING. ((G. Hummer,[1] S. Garde,[1,2] A. E. García,[1] M. E. Paulaitis,[2,3] and L. R. Pratt[1])) [1]Theoretical Division, Los Alamos National Laboratory, Los Alamos, NM 87545. [2]Center for Molecular and Engineering Thermodynamics, Department of Chemical Engineering, University of Delaware, Newark, DE 19716. [3] Department of Chemical Engineering, Johns Hopkins University, Baltimore, MD 21218.

Hydrophobic-solvation entropies of protein folding *converge* to approximately zero at a temperature of about 385 K, as measured by high-sensitivity calorimetry. The convergence behavior of solvation entropies of hydrocarbons in water is well known. However, no microscopic mechanism for these phenomena has been offered. We develop an information-theory model of hydrophobic effects that is used to explain this behavior on a *molecular* basis [1]. The entropy convergence follows directly from the density and density fluctuations of liquid water. The entropy at convergence is predicted to be negative. This affects the extraction of entropic contributions to protein folding beyond non-polar hydration by extrapolation to the convergence temperature; and it helps to infer structural properties of proteins based on thermodynamic information from calorimetric measurements.

[1] G. Hummer, S. Garde, A. E. García, A. Pohorille, L. R. Pratt, *Proc. Natl. Acad. Sci. USA* **93**, 8951-8955 (1996).

M-PM-C2

KINETIC STUDIES OF THE SELF-ASSEMBLY OF THIOREDOXIN FRAGMENTS (1–73, 74–108): A MODEL SYSTEM FOR ASSOCIATION/FOLDING PROCESSES. ((Alain Chaffotte, Jian-Hua Li, Michel Goldberg and **María Luisa Tasayco**)) Chemistry Department, The City College of the CUNY, New York, NY 10031.

The isolated fragments of *E. coli* thioredoxin (1–73, 74–108) are essentially in the random coil state. These fragments have competent conformations that undergo an association/folding process which reconstitutes the overall structure of the native protein. The kinetic measurements of this reconstitution under pseudo-first order conditions indicate a second order rate constant $k_{on} = 1,308 \pm 13\ M^{-1}s^{-1}$ and two first order rate constants $k_1 = 0.045 \pm 0.015\ s^{-1}$ and $k_2 = 0.0021 \pm 0.0006\ s^{-1}$. The second order phase involves a parallel recovery of the overall secondary structure and the tertiary structure around the Trp residues, implying the coupling of fragment association with folding. A comparison of the kinetics of refolding of thioredoxin (Trx) with the reconstitution of Trx shows the same two first order rate constants. The presence of the slowest first rate constant in both cases suggest that the formation of the native-like non covalent complex requires the slow trans-cis peptidyl-prolyl isomerization at position 76. Interestingly, the isomerization step within the C-fragment (74–108) is coupled to an isomerization within the N-fragment (1–73). The non-covalent complex undergoes a multiphasic dissociation/unfolding process which is compatible with a preferential isomerization of the complex previous to dissociation. Both steps are denaturant dependent and give by extrapolation the values $k_{-1} = 7.25 \times 10^{-4}s^{-1}$ and $k_{-2} = 3.87 \times 10^{-5}s^{-1}$ for the first order rate constants in the absence of denaturant. Our results indicate that further kinetic studies with these fragments might reveal the mechanism of inter as well as intramolecular recognition.

M-PM-C3

SOLVENT DESTABILIZATION OF PROTEINS ((C. M. Phillips, A. Sytnik and R. M. Hochstrasser)) Department of Chemistry and Regional Laser and Biotechnology Laboratories, University of Pennsylvania, Philadelphia, PA 19104-6323.

By creating a laser-based temperature jump in an aqueous protein solution [Phillips, et al., 1994; *Biophys. J.* **66**, A398; Phillips, et al., 1995; *Biophys. J.* **68**, A131] we have induced conformational changes and monitored the transient Amide I infrared spectrum of Ribonuclease A, which mimics the equilibrium infrared spectrum of the fully denatured form [Phillips, et al., 1995; *Proc. Natl. Acad. Sci.* **92**, 7292-7296]. In contrast to these results, preliminary experiments on the thermal denaturation of the ribonuclease in *Bacillius Amyloliquefaciens* (Barnase) reveal a transient spectrum which is dramatically different from that of the equilibrium spectrum. In addition, there is a fast process (~400 ps) in which measurable changes occur in the β-sheet region of the Amide I spectrum (1630 cm^{-1}). We attribute these changes to solvation of the normally hydrophobic regions of the protein and disruption of H-bonding in these structures and that "squeezing" water out of these regions is the final step in folding. Our temperature jump methodology has been extended into the μs and ms time regimes to form a complete dynamic picture of the conformational changes in these proteins.

Supported by NIH grant RR 01348.

M-PM-C4

CYTOCHROME *c* FOLDING INITIATED BY SUBMILLISECOND MIXING AND PROBED BY RESONANCE RAMAN SCATTERING ((Syun-Ru Yeh[1], Satoshi Takahashi[2], Tapan K. Das[1], Baochen Fan[1], David S. Gottfried[1] and Denis L. Rousseau[1])) 1: Department of Physiology and Biophysics, Albert Einstein College of Medicine, Bronx, NY 10461; 2: The Institute of Physical and Chemical Research (RIKEN), Wako, Saitama 351-01, JAPAN

Cytochrome *c* (cyt. *c*) folding was initiated by diluting the denaturant-unfolded protein in a submillisecond solution mixer with a dead time of ~100 μs, and investigated by resonance Raman scattering. The heme ligation processes were identified in the high frequency region of the spectra and found to exhibit large time dependent changes. The spectra were deconvoluted into contributions from the native His-Met coordination (HM), a bis-His form (HH) and a His-water form (HW). A kinetic model is proposed based on a three-state mechanism, suggesting that the folding process involves two distinctive steps: a burst phase appearing within the mixing dead time is followed by a ligand exchange phase. The spectra in the low frequency region shows a steady progression of native tertiary structure formation near the heme pocket coincident with the formation of HM, indicating that the two processes are concerted. When the pH was reduced from 5.9 to 4.5, the rate of formation of the mis-folded HH form decreased by two orders of magnitude due to the protonation of His. The energetics of the folding suggest that the high activation energy barrier for cyt. *c* to escape from its mis-folded HH form prevents the protein from folding rapidly. In the absence of wrong bond formation cyt. *c* can fold into its native structure with a rate constant of 507 s^{-1}.

M-PM-C5

EQUILIBRIUM CONSTANTS AND FREE ENERGIES IN UNFOLDING OF PROTEINS IN UREA SOLUTIONS. (I. M. Klotz)

Northwestern U., Evanston, IL 60208-3113

A novel thermodynamic approach to the reversible unfolding of proteins in aqueous urea solutions has been developed based on the premise that urea ligands are bound cooperatively to the macromolecule. When successive stoichiometric binding constants have values larger than expected from statistical effects, an equation for moles of bound urea can be derived that contains imaginary terms. For a very steep unfolding curve, one can then show that the fraction of protein unfolded, $\overline{B}$, depends on the square of the urea concentration, U, and is given by

$$\overline{B} = \frac{A_1^2 e^{\lambda n \overline{B}} U^2}{1 + A_1^2 e^{\lambda n \overline{B}} U^2}$$

where A_1^2 is the binding constant as $\overline{B} \rightarrow 0$, and λ is a parameter that reflects the augmentation in affinities of protein for urea as the moles bound increases to the saturation number, n. This equation provides an analytic expression that repro-duces the unfolding curve with good precision, suggests a simple linear graphical procedure for evaluating A_1^2 and λ, and leads to the appropriate standard free energy changes. The calculated ΔG° values reflect the coupling of urea binding with unfolding of the protein. Some possible implications of this analysis to protein folding *in vivo* are described.

M-PM-C6

EARLY EVENTS IN PROTEIN FOLDING STUDIED BY PHOTOINITIATION OF α-HELIX FORMATION IN *DE NOVO* PEPTIDES

((M. Volk,* Y. Kholodenko,* E. Gooding,* H. Lu, W.F. DeGrado, and R.M. Hochstrasser*))
*Dept. of Chemistry and School of Medicine, Univ. of Pennsylvania, Philadelphia, PA 19104 USA

Recently, it has been shown that folding and unfolding of secondary structural elements of proteins can occur on the time scale of 10-100 ns [1,2]. For the investigation of the early events of α-helix formation, we designed a series of short, purely α-helical peptides which are constrained to a "non-native", more randomly coiled conformation by a disulfide bond between the peptide ends. The ease of changing the structure and sequence of *de novo* designed peptides will enable us to answer specific questions about the mechanism of α-helix formation. The ultrafast triggering event necessary for the study of fast folding is achieved by photodissociation of the disulfide bond.

Transient absorbance measurements with sub-ps time resolution show the fast splitting of the disulfide bond, resulting in the formation of thiyl radical pairs. The anisotropy of the radical absorbance around 600 nm decays with a time constant of 200 ps, corresponding to the rotational diffusion of the peptide. It can be concluded that no significant internal peptide motions occur before 200 ps.

Transient IR measurements show an instantaneous bleach of the amide I band which decays parallel to the recombination of the thiyl radical pairs. This bleach is assigned to the vibrational Stark effect due to internal electric fields, arising from intramolecular charge transfer from the thiyl radicals to neighbouring amino groups. No significant shift of the amide I band, indicative of α-helix formation in short peptides [2], is observed within 2 ns after photodissociation.

The recombination dynamics of the thiyl radical pairs, measured for delay times t from 1 ps to 10 μs, is approximately described by a stretched exponential with an exponent of 0.08 and an average lifetime of 3 μs. The instantaneous rate of the radical recombination decays approximately with $1/t$ over the whole range, i.e. over 7 orders of magnitude in time. This self-similar recombination could be a consequence of the fact that the diffusional dynamics of the peptide chain is being continuously modified by the formation of the α-helix.

[1] Phillips et al., Proc. Natl. Acad. Sci. USA 92, 7292 (1995). [2] Williams et al., Biochem. 35, 691 (1996).

M-PM-C7

SPECTRAL AND KINETIC EVIDENCE OF STRUCTURAL INHOMOGENEITY IN APOMYOGLOBIN: FLEXIBLE AND STABLE MOIETIES.

((R. Gilmanshin†, R. Callender†, R.B. Dyer‡, S. Williams‡, and W.H. Woodruff‡)) †Department of Physics, City College of New York, New York, NY 10031 and ‡CST-4, Los Alamos National Laboratory, Los Alamos, NM 87545.

Temperature-induced structural changes of different forms of apomyoglobin (apoMb) were studied at various pHs and salt concentrations. Both equilibrium transitions and T-jump induced relaxations were measured using intrinsic fluorescence and IR absorbance as probes. The component of amide I' in the range 1634-1645 cm^{-1} has been assigned to "solvated" helices typical of α-helical peptides and destabilized α-helical proteins in D_2O. This band in apoMb increases with decreasing pH and increasing salt concentration. Its intensity changes monotonically with temperature and its relaxation is fast (tens of ns), analogous to the behavior of short peptide helices. Another amide I' component at 1648-1650 cm^{-1} is characteristic of α-helices within native proteins. Changes associated with this band are highly cooperative and occur with a time constant of 100 μs, after unfolding of the "solvated" helices. The maximum of the intrinsic tryptophan fluorescence spectrum is 332-336 nm throughout the temperature range measured for most conditions. This suggests that the apoMb tryptophans are substantially screened from solution, since completely exposed tryptophan emits with a spectral maximum of 346 nm. Both tryptophans of apoMb belong to the N-terminal A-helix, hence, it is likely that the AGH helical complex remains folded under most conditions. Only for conditions which produce a greatly expanded state (pH*3, low ionic strength) and high temperature, does the fluorescence indicate unfolding of the tryptophans' surrounding. Our results demonstrate coexistence of different substructures within the apoMb molecule which have different thermodynamic and kinetic properties.

M-PM-C8

RAPID CONDENSATION OF HYDROPHOBIC CLUSTERS AND SLOW ACTIVE SITE FORMATION IN STAPHYLOCOCCAL NUCLEASE FOLDING.

((T.Y. Tsong[1,2] and Z.D. Su[1])). 1: Biochem, Hong Kong Univ of Sci & Technol, Kowloon, Hong Kong, and 2: Biochem, U of Minn, St. Paul, NM 55108 (Spon. by D. C. Chang)

Folding of *staph.* nuclease (SNase) has been shown to follow a least activation path which is composed of 3 sub-states of the unfolded protein and 1 native state. Each of the 4 kinetic species is composed of 2 forms, one with Pro117 in the cis-isomeric, and the other in the trans-isomeric forms. By stopped-flow double jump technique monitoring the regeneration of the nuclease activity and the formation of the hydrophobic clusters which bind the fluorescence probe, ANS, we have detected two additional folding intermediates. GdmCl (2.2 M)-unfolded SNase was diluted to 0.2 M in the first jump. After a time interval (t_D), ANS in 0.2 M GdmCl was mixed with the protein sample in the second jump. Initial rate of ANS binding was plotted vs. t_D to obtain kinetics of the condensation of the hydrophobic clusters. A 100 ms reaction was resolved. By a similar method, kinetics of the active site formation was shown to occur in 35 s for folding at 0.2 M GdmCl, and of loss of enzyme activity was shown to occur in 0.06 s for unfolding at 2.2 M GdmCl. Thermodynamic and kinetic properties of these intermediates have been determined. All folding intermediates we have observed so far are either close to the unfolded protein or close to the native state in conformational stability. No folding intermediates of medium stabilities have been detected.

M-PM-C9

STRUCTURAL BASIS OF THE EXTREME STABILITY OF RIBONUCLEASE P2 FROM THERMOPHILIC *SULFOLOBUS SOLFATARICUS*.

((E. Mombelli[a], P. Tortora[b] and **R. Lange[a]**)) [a]INSERM U128, Montpellier, France and [b]Dipartimento di Fisiologia e Biochemical generali, Università di Milano, Milano, Italy (Spon. by C. Tetreau)

Ribonuclease P2 (7 kDa) is extremely stable towards high temperature (>90 °C) and high pressure (>700 Mpa). However, it is sensitive to lower temperatures and at 200 Mpa and at -20 °C a reversible cold denaturation occurs. The nature of the structural changes was assessed by 4th derivative UV spectroscopy, a technique which allows selective enhancement of specific spectral bands of tyrosine and tryptophan residues in various environments, and which can be used to evaluate changes of the mean dielectric constant near these residues when they become more exposed to the solvent due to changes in protein conformation.

This small protein (7 kDa) turned out to be a suitable model for the study of differences of protein conformational states. Results with mutant forms (F31A and F31Y) suggest that the structural basis of the stability of this protein is connected to the presence of an aromatic cluster in its hydrophobic core. As shown by the UV spectra, temperature and pressure induced distinctly different protein structural changes. Furthermore, the effect of these parameters on the core aromatic interactions could be studied. Low temperatures and high pressures appeared to exert opposite effects.

M-PM-D1

ANOMALOUS L-TYPE CALCIUM CHANNELS OF RAT SPINAL MOTONEURONS. ((B. Hivert and **D. Pietrobon**)) Dept. Biomedical Sciences, CNR Center Biomembranes, University of Padova, 35121 Padova, Italy.

Single channel recordings show that E15 rat spinal motoneurons in primary culture express three functionally different subtypes of dihydropyridine (DHP)-sensitive calcium channels. The most abundant L subtype opens very rarely in control conditions (nearly zero p_O), and its prevailing mode of activity in the presence of DHP agonist is characterized by a peculiar fast inactivation (with τ ranging from 50 to 150 ms at +10 mV, 90 mM Ba^{2+}) and by relatively short openings (t_O=5 ms). This 24 pS L-type channel can occasionally shift to a high-po non-inactivating mode with long openings (t_O=20 ms). The time spent in the high-po mode as well as availability and rate of inactivation are modulated by a biochemical pathway, possibly involving phosphorylation of the channel. In addition, motoneurons express L-type channels with lower conductance (20 pS) and anomalous gating similar to those of cerebellar granule cells (Forti and Pietrobon 1993, Neuron 10, 437-450). Also these channels have nearly zero open probability in control conditions. Their gating anomalies are i) p_O and average open time decreasing with increasing voltage above +20 mV (p_O=0.08, t_O=2 ms at +20 mV and p_O=0.02, t_O=0.8 ms at +40 mV in the presence of DHP agonist), and ii) multiple long reopenings upon repolarization (t_O=5 ms at -30 mV), whose frequency of observation increases with the amplitude of the preceding depolarization. Reopenings are not due to recovery from inactivation since anomalous L-type channels do not inactivate during depolarizations that induce reopenings (holding potential = -100 mV). The gating anomalies can be explained by a model in which voltage controls the equilibrium between particular gating modes.

(Supported by Telethon, Italy, n. 720).

M-PM-D2

β-SUBUNIT MODULATION OF G-PROTEIN INHIBITION AND VOLTAGE-DEPENDENT INACTIVATION OF P/Q-TYPE (A-CLASS) NEURONAL CALCIUM CHANNELS

((**Parag G. Patil**, David L. Brody, Terry P. Snutch, and David T. Yue))
Dept. of Biomedical Engineering, Johns Hopkins University, Baltimore, MD 21205

P/Q-type (A-class) calcium channels are widely distributed in brain and are believed to initiate synaptic transmission at a variety of central synapses. G-protein-mediated inhibition of these channels reduces presynaptic calcium entry, sharply attenuating neurotransmitter release. Biochemical studies suggest that A-class channels result from combinations of α_{1A}, α_2, and one of several different β subunits. To explore the functional implications of β subunit diversity on A-class channels, we co-transfected HEK 293 cells with A-class channels (α_{1A}+α_2+one of four β subunit isoforms) and an M2-muscarinic receptor. As expected from previous studies, the identity of the β subunit had significant effects on voltage-dependent inactivation. Under control conditions (**O**), channels with β_{1b} inactivated far more rapidly than those with β_{2a} during a 100 ms test pulse to +20 mV. Furthermore, during G-protein inhibition (50μM carbachol), the β subunit affected channel responses to test pulses alone (+) and following a 100 mV prepulse (*). Channels with β_{1b} showed far less kinetic slowing for the extent of inhibition and little reversal of inhibition by the prepulse, compared to those with β_{2a}. Hence, β subunit modulation of both G-protein inhibition and voltage-dependent inactivation may importantly affect action-potential evoked calcium entry and neurotransmitter release at central synapses.

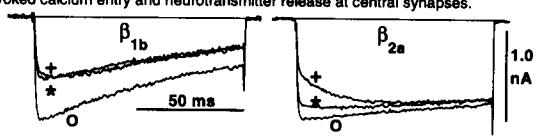

M-PM-D3

CROSSTALK BETWEEN PKC-DEPENDENT UPREGULATION AND DIRECT G-PROTEIN INHIBITION OF N-TYPE Ca CHANNELS IS MEDIATED BY THE Ca CHANNEL DOMAIN I-II LINKER. ((**G. W. Zamponi**, E. Bourinet, D. Nelson, J. Nargeot, and T. P. Snutch)) University of British Columbia, Biotechnology Laboratory, 6174 University Boulevard, Vancouver V6T 1Z3, Canada.

The modulation of voltage-gated Ca channels at presynaptic nerve terminals is a key factor in controlling neurotransmitter release and synaptic function. Many neurons express both N-type (α_{1B}) and P/Q-type (α_{1A}) Ca channels at their presynaptic terminals. In intact neurons and when expressed transiently in *Xenopus* oocytes or HEK cells, these Ca channel isoforms are differentially regulated by PKC stimulation and by activation of G-protein βγ subunits. Crosstalk between these two second messenger systems has been reported in neurons, where PKC-dependent phosphorylation attenuates direct G-protein inhibition. We addressed the mechanism underlying crosstalk using several approaches. To approximately identify the region involved in G-protein interaction, we tested the response of wild type and chimeric Ca channels to stimulation of G-protein coupled receptors. To confirm a direct interaction between G proteins and the Ca channel α_1 subunit, we examined binding of radiolabelled $G_{\beta\gamma}$ subunits to fusion proteins directed against various regions of the α_{1B} channel. To more precisely identify the targets of G-protein binding, we performed patch clamp recordings on HEK cells expressing α_{1B} in which the patch pipette contained purified $G_{\beta\gamma}$ together with a series of synthetic peptides against regions of the α_{1B} and α_{1A} subunits. Finally, to examine the mechanism underlying crosstalk, any peptides which both inhibited G-protein interactions and contained PKC consensus sites were phosphorylated *in vitro* and added to the patch pipette together with $G_{\beta\gamma}$. The experiments identified two distinct regions within the Ca channel domain I-II linker which bind $G_{\beta\gamma}$, one of which overlaps with the binding site for the Ca channel β subunit, and a second site approximately 30 amino acid residues downstream which is also a substrate for PKC. Phosphorylation of this site dramatically attenuates $G_{\beta\gamma}$ interaction and we propose that crosstalk results from a competitive interaction between direct $G_{\beta\gamma}$ binding and the PKC-dependent phosphorylation of residues in the domain I-II linker.

M-PM-D4

G-PROTEIN MODULATION OF N-TYPE Ca^{2+} CHANNEL GATING CURRENTS

((**L.P. Jones***, P. Patil*, T.P. Snutch† and D.T. Yue*)) *Johns Hopkins Univ., Baltimore, MD 21205; †Univ. of British Columbia, Vancouver, Canada, V6T 1Z3

Voltage-dependent inhibition of N-type Ca^{2+} currents by G proteins contributes importantly to presynaptic inhibition, yet key features of the mechanism by which G proteins produce this effect remain unclear. Only limited inferences about the intermediary transitions preceding channel opening have been possible through ionic current measurements. Here, N-type gating currents are clearly isolated, enabling the direct measurement of the effect of G proteins on the voltage dependent transitions that correspond to voltage sensor movement. N-type currents were expressed in HEK 293 cells transiently transfected with α_{1B}+β_{1b}+α_2. Voltage-dependent inhibition was reconstituted during dialysis with GTPγS: as expected, strong depolarizing prepulses increased ionic currents, and left-shifted the voltage-dependent activation of ionic current (compare *G-V* curves in A vs. B). No such effects were observed with GDPβS. Using 0.1 mM free La^{3+} to isolate gating currents, G protein activation could now be seen to inhibit gating currents and to produce depolarizing shifts in the voltage dependent activation of gating charge movement. Strong depolarizing prepulses largely reversed these effects (compare *Q-V* curves in A vs. B). Even more striking was the induction of a ~20 mV separation between the *Q-V* and *G-V* curves by G proteins (B) which was largely eliminated by a depolarizing prepulse (A). These results provide strong indications that G proteins act to inhibit both voltage-sensor movement and the transduction of voltage-sensor activation into channel opening.

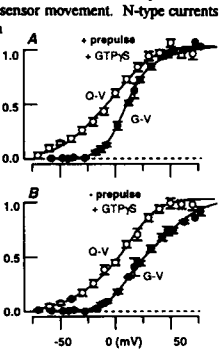

M-PM-D5

BURSTS OF ACTION POTENTIAL-SHAPED VOLTAGE WAVEFORMS CAN RELIEVE G-PROTEIN INHIBITION OF RECOMBINANT A-CLASS Ca^{2+} CHANNELS.

((**D. L. Brody**, P. G. Patil, J. G. Mulle, T. P. Snutch, and D. T. Yue)) The Johns Hopkins University, Department of Biomedical Engineering, Baltimore, MD 21205.

A variety of neurotransmitters acting through G-protein coupled receptors decrease synaptic transmission largely by inhibiting the voltage-gated calcium channels that trigger neurotransmitter release. We have reconstituted a part of this inhibition using recombinant A-class calcium channels and M2 acetylcholine receptors which couple to the endogenous G-proteins in HEK293 cells. This inhibition shows many features seen in native neurons. We have found that short bursts of action potential-shaped voltage waveforms can partially relieve the inhibition, increasing current through G-protein inhibited channels (figure) but not through uninhibited channels. The extent of this relief as well as the overall size of the currents depended strongly on the duration of the action potential- shaped voltage waveforms. This is the first direct evidence favoring the possibility that relief of G-protein inhibition might occur during high-frequency trains of action potentials. This effect may contribute to short term changes in synaptic efficacy that are sensitive to action potential timing and duration. Even modest changes in calcium entry may have strong effects on neurotransmitter release, since synaptic efficacy is proportional to $[Ca]_i^{\,n}$ where n has been measured as high as 4.

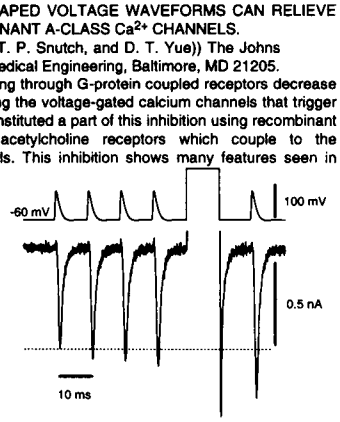

M-PM-D6

STABILITY OF G PROTEIN-MEDIATED INHIBITION OF Ca^{2+} CURRENT MODULATED BY KINASE-PHOSPHATASE BALANCE IN PARASYMPATHETIC NEURONS.

((**James E. Simples, Jr.**, Michael G. White & Stephen D. Meriney))
Department of Neuroscience, University of Pittsburgh, Pgh, PA 15260

Somatostatin-induced G protein inhibition of N-type Ca^{2+} channels in stage 40 parasympathetic chick ciliary ganglion neurons was studied using the perforated patch technique. The characteristics of somatostatin-mediated inhibition are dependent on the activity of a nitric oxide (NO)-cGMP dependent protein kinase pathway. Under conditions that support the activity of this pathway, somatostatin inhibition is characterized by slow desensitization and modulated current that does not display kinetic slowing. Following blockade of the NO-cGMP pathway, somatostatin inhibition desensitizes rapidly and modulated current displays kinetic slowing (Meriney et al., 1994, Nature, 369: 336-9). We have tested the hypothesis that the sensitivity to strong voltage prepulses of somatostatin-mediated inhibition of calcium current is altered by the kinase-phosphatase balance in these cells. In control cells, voltage prepulses (to +80 or +100 mV for 30 msec) relieved only 51 ± 2% (mean + SEM; n= 8) of the somatostatin-mediated inhibition. Following blockade of the NO-cGMP pathway with 1-10 mM L-NAME (a NO synthase inhibitor), prepulse relief of inhibition increased to 66 ± 2% (n=19). Furthermore, in cells treated with L-NAME, prepulses relieved modulated Ca^{2+} current that was characterized by slowed activation kinetics. Modulated Ca^{2+} current that was resistant to prepulse relief desensitized slowly and was not characterized by slowed activation kinetics. We conclude that somatostatin modulates N-type Ca^{2+} channels in ciliary ganglion cells through a voltage-dependent mechanism, and that the NO-cGMP pathway modulates the stability (or resistance to strong voltage prepulses) of the voltage-dependent modulation. Supported by AHA 96012640 and NIH NS 32345.

M-PM-D7

CHARACTERIZATION OF INTERACTION DOMAINS BETWEEN THE VOLTAGE-DEPENDENT CALCIUM CHANNEL $\alpha_2\delta$ AND α_1 SUBUNITS. ((**Christina A. Gurnett,** Ricardo Felix, and Kevin P. Campbell)) Howard Hughes Medical Institute and Department of Physiology and Biophysics, University of Iowa College of Medicine, Iowa City, IA 52242

Voltage-dependent Ca^{2+} channels are modulated by complex interactions with their auxiliary subunits. We previously identified domains required for the functional effects of the Ca^{2+} channel $\alpha_2\delta$ subunit on current amplitude. Using transiently transfected tsA201 cells, we have now investigated the sites responsible for structural interactions between this auxiliary subunit and the ion pore. Transfected tsA201 cells processed the $\alpha_2\delta$ subunit properly as disulfide linkages and cleavage sites between the α_2 and δ subunits were preserved. Transfection of the $\alpha_2\delta$ with the α_{1S} subunit did not increase the amount of α_{1S} protein as determined by western blot analysis and [^{3}H] PN-200-110 binding. Immunoprecipitation experiments demonstrated that α_2 cannot be coimmunoprecipitated with the α_1 subunit in the absence of the δ subunit. However, the transmembrane sequence in δ can be exchanged with that of an unrelated protein without any effect on the interaction between these proteins. This suggests that the nontransmembrane regions of δ are responsible for associating with the α_1 subunit. Investigation of the corresponding interaction site on the α_1 subunit revealed that while tryptic peptides containing repeat III of native α_{1S} remains in association with the $\alpha_2\delta$ subunit during WGA chromatography, repeat III by itself is not sufficient for association with the $\alpha_2\delta$ subunit. We conclude that the $\alpha_2\delta$ subunit likely interacts with more than one extracellular loop of the α_1 subunit.

M-PM-D8

DIRECT INTERACTION BETWEEN VOLTAGE-DEPENDENT CA^{2+} CHANNELS AND G PROTEIN $\beta\gamma$ COMPLEX. ((**H. Liu,** M. De Waard, R. Felix, K.P. Campbell)) HHMI, Program in Neuroscience and Department of Physiology and Biophysics, University of Iowa, Iowa City, IA 52242

Neurotransmitters and hormones regulate the efficacy of synaptic transmission by inhibiting the function of neuronal voltage-dependent Ca^{2+} channels via their G protein coupled receptors. Previously it has been shown that presence of Ca^{2+} channel β subunit exerts antagonistic effects to the modulation of Ca^{2+} channels by heterotrimeric G proteins. We have identified a direct interaction of the G protein $\beta\gamma$ complex with α_{1A} subunit of P/Q- Ca^{2+} channels. The binding of $G\beta\gamma$ occurs on two sites wthin the I-II cytoplasmic linker of α_{1A} subunit. One of these site is the alpha$_1$ interaction domain (AID), a region essential for anchoring the Ca^{2+} channel β subunit, and the other is in a downstream sequence (D2) within the I-II linker. Several N-terminal AID residues are critical for $G\beta\gamma$ binding, whereas C-terminal AID residues have been previously shown to be essential for Ca^{2+} channel β interaction. Mutation of the R387 residue in AID eliminated the binding of $G\beta\gamma$ to this site and likewise abolished G protein modulation of this channel expressed in *Xenopus* oocytes. Our data demonstrate that the $G\beta\gamma$ complex interacts with the P/Q-type Ca^{2+} channels through two domains (AID and D2) in the I-II linker of α_{1A} subunit.

M-PM-D9

FUNCTION OF CALCIUM CHANNEL β SUBUNITS IN CARDIAC MYOCYTES. ((**A.E. Lacerda**)) Rammelkamp Campus, MetroHealth Medical Center, Case Western Reserve University, Cleveland, OH

Voltage gated calcium channels are comprised of a pore forming subunit and up to four additional accessory subunits that vary among tissues. Evidence from heterologous expression studies suggest that all the cloned calcium channel subunits have functional roles in the calcium channel complex. The β subunits are known to modulate the activation and inactivation kinetics and voltage dependence of expressed calcium channel currents and their magnitudes. Although all heterologous expression systems in which calcium channel subunits have been coexpressed show some effect of β subunits on the expressed currents, the effects vary between expression systems. One approach to determine the functional role of calcium channel subunits in the cells in which they are expressed is to specifically alter the expression of a targeted subunit. Antisense oligonucleotides can specifically suppress the expression of targeted genes. Antisense oligonucleotides targeted to a sequence common to all cloned β subunits was either added to the media of cultured neonatal rat myocytes or microinjected into myocytes. After two days significant effects on current magnitude and the availability of calcium channels were observed relative to cultures treated with antisense oligonucleotides with the same chemical composition but randomized sequence. An approximately five-fold reduction in current magnitude and a ten mV right-shift in channel availability occurred.

M-PM-D10

CHARACTERIZATION OF THE PHOSPHODIESTERASE ISOFORMS INVOLVED IN THE COMPARTMENTATION OF cAMP FOLLOWING β-ADRENOCEPTOR ACTIVATION IN FROG CARDIAC MYOCYTES. ((J. Jurevicius, A. Skeberdis and **R. Fischmeister**)) INSERM U-446, Univ. Paris-Sud, 92296 Châtenay-Malabry, France.

We have shown recently that stimulation of the L-type calcium current (I_{Ca}) with isoprenaline (ISO) is accompanied by a strong cAMP subcellular compartmentation in frog ventricular myocytes (*PNAS* **93**, 295-299, 1996). Using the extracellular micro-perfusion technique (*J. Physiol. (Lond.)* **492**, 669-675, 1996), we have now investigated the role of phosphodiesterase (PDE) isoforms in this process. We measured the *local* and *distant* effects of ISO (100 nM) on I_{Ca} in the presence of nimodipine (1-10 μM), milrinone (3 μM) and RO 20-1724 (3 μM), to selective inhibit PDE1, PDE3 and PDE4, respectively. The effects of these compounds were compared to that of IBMX (100 μM), a non-selective PDE inhibitor. PDE3 or PDE4 inhibition increased the *distant* effect of ISO by $\approx$3-fold, i.e. $\approx$50% as much as IBMX. PDE1 inhibition had no effect unless the internal medium was preserved using the perforated patch configuration (nystatin 200 μg/ml). cAMP-dependent phosphorylation appeared not to be involved in the mechanism of activation of PDE3 and PDE4 because okadaic acid (3 μM), a phosphatase inhibitor, and H-89 (1 μM), a protein kinase inhibitor, had no influence on the *distant* effect of ISO. We conclude that upon activation of β-adrenoceptors, cAMP is used locally for activation of nearby Ca^{2+} channels and that little amount of cAMP diffuses in the cytosol mainly because of a strong activity of PDE3 and PDE4.

MICROSCOPY

M-PM-E1

DIRECT VISUALIZATION OF THE ROTATION OF F_1-ATPASE ((**R. Yasuda**[1],H. Noji[2], K. Kinosita, Jr.[1], and M. Yoshida[2])) [1]Dept. Phys., Fac. Sci. Tech., Keio Univ., Hiyoshi 3-14-1, Yokohama 223, Japan: [2]Res. Lab. Resources Utilization, Tokyo Inst. Tech. Nagatsuda 4259, Yokohama 226, Japan.

The H^+-ATPase is made of two units, F_0 which spans the membrane and mediates proton translocation, and F_1 which catalyzes ATP hydrolysis. According to the binding change hypothesis, rotation of the γ subunit in F_1 couples ATP hydrolysis (or synthesis) with proton translocation. To observe directly the rotation of the γ subunit, we attached a fluorescently labeled actin filament to the γ subunit in F_1 immobilized on a glass surface. In the presence of ATP, rotating actin filaments were observed under an epifluorescence microscope. Some filaments rotated continuously for more than 100 revolutions. The rotation was always in the same direction: anti-clockwise when viewed from the F_0 (membrane) side. The rotation rate was 0.2-4 revolutions per second, and in general, smaller when the attached actin filament was longer. The torque against viscous friction was estimated to be up to ~40 pN·nm. In the presence of azide, which is an inhibitor of ATPase activity, or in the absence of ATP, no rotating filament was found.

M-PM-E2

INTERMOLECULAR INTERACTION FORCE MEASURED BETWEEN APOPROTEIN(A) AND ITS LIGAND LYSINE WITH SCANNING (ATOMIC) FORCE MICROSCOPY. ((Shaohua Xu and Morton F. Arnsdorf)) Dept. of Medicine, University of Chicago, Chicago, Ill 60637. (Spon. S. Shroff)

The intermolecular interaction force between apoprotein(a), apo(a), and lysine was measured with scanning (atomic) force microscopy (SFM). Apo(a), part of the atherothrombogenic lipoprotein(a), consists of one strong and two weak lysine binding sites. We covalently bonded apo(a) to a Si_3N_4 tip and lysine to both sepharose beads and glass cover slips. The interactions of apo(a)-tip with lysine-sepharose beads and with lysine-glass were monitored. The adhesion force between the apo(a)-tip and the lysine-sepharose beads was so large that the apo(a)-tip could actually drag the lysine-sepharose beads around and off the glass substrate on which the beads rested. Addition of 250 mM ϵ-amino-n-caproic acid and 200 mM NaCl blocked the binding of the lysine beads to the tip. The ϵ-amino-n-caproic acid competes for the lysine binding sites of the apo(a). Glass cover slips activated with excess lysine (50 mM) showed very small adhesion force ($F_{ad}<2$ nN). In contrast when the glass cover slip was activated with less lysine (1 mM), a large adhesion force was observed ($F_{ad}=8.4$ nN, n=50) when measured in 250 mM NaCl, 10 mM sodium phosphate buffer, pH 7.4. This adhesion force reduced to less than 1 nN when the NaCl was replaced with 250 mM of ϵ-amino-n-caproic acid. The adhesion force between the apo(a)-tip and the lysine-glass cover slip seems to be directly related to the NaCl concentration. The work presented shows the potential of SFM in the study of molecular pharmacology and in the basic understanding of intermolecular interactions.

M-PM-E3

DETAILS OF LIPID MOTION IN BIOMEMBRANES STUDIED BY SINGLE MOLECULE MICROSCOPY *.

((G.J. Schütz, H. Schindler and Th. Schmidt)) Institute for Biophysics, University of Linz, Altenberger Str. 69, 4040 Linz, Austria.

Single molecule microscopy is employed to study lipid motion in artificial biomembranes. The lateral mobility of individual lipids in supported phospholipid membranes clearly shows biphasic behaviour which is interpreted in terms of the mobile and immobile fraction often found in FRAP experiments. In contrast to latter results it is shown that the "*immobile*" fraction exhibits diffusional motion hindered by local restrictions. The potential of such single molecule techniques in combination with a newly developed analysis, relying on the determination of the probability function of square displacements, is shown for lateral motion in a polymer-stabilized monolayer. Local restrictions on the length scale of ~100nm were directly visualized. Further, correlations of lateral with rotational mobility, as determined by the linear dichroism on the single molecule level, are discussed for various systems.

(Supported by the Austrian Research Funds, project S06607-MED)

M-PM-E4

FRET MICROSCOPY ON FLUORESCENT LABELED CHOLERA TOXIN; INTRACELLULAR TRAFFICKING AND PROCESSING.

((**P.I.H. Bastiaens**, L. Erijman, I.V. Majoul and T.M. Jovin)) Department of Molecular Biology, Max Planck Institute for Biophysical Chemistry, P.O. Box 2841, 37018 Göttingen, Germany.

Cholera toxin (CTX) from *Vibrio cholerae* has an AB_5 oligomeric structure consisting of one 27.3 kDa A subunit (CTA) embedded in an isopentamer of 11.7 kDa B subunits (CTB). The holotoxin binds to cell surface via interactions of CTB with ganglioside G_{M1}. After internalization CTB and CTA dissociate, followed by reductive cleavage of CTA with liberation of the enzymatically active 21.8 kDa A1 peptide which ADP-ribosylates the α subunits of heterotrimeric G_s proteins. We have applied preparative high pressure techniques to uniquely label the B and A subunits with the sulfoindocyanine dyes Cy5 and Cy3 respectively. This approach allows the observation of the trafficking of the individual subunits within the cell by multichannel confocal microscopy[1]. In addition, the Cy3-Cy5 chromophores form a donor-acceptor pair exhibiting fluorescence resonance energy transfer (FRET) with a critical distance of 50% transfer (R_0) of 5 nm. By measuring FRET in the microscope with fluorescence lifetime imaging (FLIM) or photochemical digital imaging microscopy (pcDIM), information on the quaternary structure of CTX within subcellular compartments is obtained. In this way it was determined that CTX is transported in vesicular structures from the plasma membrane to the Golgi which is the cellular locus of CTA and CTB separation. The CTA subunit is transported via a retrograde mechanism to the ER from which it presumably translocates to the cytosol. This mechanism is under current investigation.

1. Bastiaens, P. I. H. *et al* 1996. *EMBO J.* 15:4246-4253.

M-PM-E5

INFRARED SPECTROSCOPIC IMAGING STUDIES OF BRAIN TISSUE DERIVED FROM THE MUTANT NIEMANN PICK C MOUSE

((**E. Neil Lewis**[1], Linda H. Kidder[1], Peter Pentchev[2], Ira W. Levin[1] and David S. Lester[3])) [1]Laboratory of Chemical Physics, NIDDK, National Institutes of Health, Bethesda MD 20892. [2]Developmental and Metabolic Neurology Branch, NINDS, National Institutes of Health, Bethesda MD 20892. [3]Center for Drug Evaluation and Research, Food and Drug Administration, Laurel, MD 20708

Since the structure and spatial distribution of components within complex materials dictate physical and chemical properties, knowledge of these intrinsic parameters is important for elucidating organizational motifs and predicting molecular behavior. Therefore, analytical techniques which simultaneously record both spatial and chemical information are invaluable diagnostic and research tools. For example, nmr spectroscopy and fluorescence spectroscopy have both evolved imaging components over their histories that are particularly suitable for microscopic analyses (fluorescence imaging) and *in vivo* biomedical diagnoses (nmr imaging). As image contrast is provided solely by spatial variations in a sample's intrinsic chemistry, the researcher and clinician can visualize a sample directly in terms of its chemical heterogeneities. We have recently developed new chemical visualization methods integrating microscopy with vibrational spectroscopic methods, including Raman, near-infrared and mid-infrared spectroscopies. These techniques rely on the use of new developments in tunable filter and infrared focal-plane array detector technologies. Using our current microscope configurations we can rapidly and simultaneously collect Raman and infrared images with data sets containing up to 16,384 spatially resolved high resolution spectra which individually sample 1-4 μm^2 of the sample surface. We have applied this chemical imaging approach to explore a number of biological problems including the study of the neurodegenerative genetic disease, Niemann-Pick C. Chemical analyses of brain tissue derived from the mutant mouse NPC indicate that there are significant changes in cholesterol transport resulting in alterations in lipid organization. We are currently undertaking infrared spectroscopic imaging studies of brain tissue slices derived from this model system to help determine localization or changes in the distribution of these cellular components in wild type and mutant strains. This and other studies will help us assess the sensitivity of infrared and Raman spectroscopy and imaging in the analysis of "pathological states".

M-PM-E6

***IN VIVO* IMAGING OF (NEURONAL) CELLS WITH A SCANNING PROBE MICROSCOPE BASED ON OPTICAL TWEEZERS AND TWO-PHOTON ABSORPTION PROCESSES**

((**Ernst-Ludwig Florin**, Arnd Pralle, J.K. Heinrich Hörber and Ernst H.K. Stelzer)) Cell Biophysics Programme, European Molecular Biology Laboratory (EMBL), Meyerhofstrasse 1, Postfach 10.2209, D-69012 Heidelberg, Germany

Recent progress in the development of a Scanning Probe Microscope (SPM) based on optical tweezers [1] enables us to image cells *in vivo*. This type of SPM relies on the mechanical contact between probe (e.g. a latex bead) and sample for image formation [2] and appropriate methods to detect the position of the probe relative to that of the laser trap.

The experiments show, that the resolution along the optical axis is given by photon statistics [1]. Under convenient conditions, we achieved an axial resolution as good as 10-15 nm. The lateral resolution is given by the size of the probe (200 nm). Mechanical deformations of the cell surfaces were found to occur already in the force range of a few piconewtons. By analyzing the image formation process, we found that the crosstalk between the lateral and axial position signal is negligible for moderate surface features, when using 2-photon fluorescence detection for position sensing. The images recorded are thus real height images, and effected by geometrical and mechanical deformation effects.

[1] E.-L. Florin, J.K.H. Hörber, and E.H.K. Stelzer. 1996. *Appl.Phys. Lett.* 69(4):446-448
[2] L.P.Ghislain, and W.W. Webb. 1993. *Optics Letters* 18:1678-1680.

M-PM-E7

PLASMA MEMBRANE WATER PERMEABILITY OF CELL LAYERS MEASURED BY PHASE CONTRAST MICROSCOPY.

((**Javier Farinas**, Megan Moore and A.S. Verkman)) Biophysics Group, UCSF, San Francisco, CA 94143.

A simple quantitative method was developed to measure the osmotic water permeability of plasma membranes in cell layers and applied to cells and epithelia expressing water channels. The method is based on the dependence of cellular refractive index on cell volume demonstrated by interferometry (Farinas and Verkman, Biophys. J. in press, 1996). A change in cell volume produces a change in the integrated intensity of transmitted monochromatic light in phase contrast microscopy. For cells of different size and shape (Sf9, CHO, A549, LLC-PK1), the transmitted light intensity was dependent on relative cell volume; generally the signal decreased 10-25% for a 2-fold increase in cell volume. A theory relating signal amplitude to cell volume was developed based on changes in optical path length caused by volume dependent changes of cellular refractive index. Theory predictions were confirmed by image analysis of cell layers. The excellent signal-to-noise ratio of the transmitted light intensity permitted measurement of cell volume changes of under 1%. The method was applied to characterize transfected cells and tissues that express water channels. Transfected CHO cells expressing aquaporins 1, 2 and 4 showed a >8-fold increase in water permeability compared to mock transfected cells. Intact mammalian epithelia were also studied. These results establish phase contrast microscopy as a technically simple and accurate method to measure relative cell volume and water permeability in cell layers and epithelia.

M-PM-E8

FAST RATIOMETRIC MEASUREMENTS OF MEMBRANE POTENTIAL USING A VOLTAGE-SENSITIVE DYE AND HIGH-SPEED, RANDOM-ACCESS, LASER-SCANNING MICRCOSCOPY.

((**Andrew Bullen** and Peter Saggau.)) Div. Neuroscience. Baylor College of Medicine. Houston, TX 77030.

A high-speed, random-access, laser-scanning, fluorescence microscope configured to make ratiometric determinations of membrane potential from small cellular structures is presented. Previously, we have described a random-access scanning system capable of high resolution (< ms, 2 µm, 16 bit) measurements from small neuronal structures (Bullen & Saggau, 1994). Here we extend this method to include the capability to make ratiometric determinations with voltage-sensitive dyes (VSD) without averaging. This approach utilizes the voltage-dependent shift in the emission spectra of the VSD, Di-8-ANEPPS. Fluorescence was elicited with a fast scanning laser source (488 nm) under computer control that was focused through a high numerical objective (Fluar, 100x: Zeiss). Emission light was collected using an epifluorescence configuration and further processed by a secondary dichroic mirror (580 nm) and two emission filters (550/50 nm & OG590). The ratio of fluorescence intensities at these wavelengths was used to generate a quantitative measurement of membrane potential that is independent of localized differences in dye staining, emission intensity and bleaching. Calibration of this ratio was achieved using simultaneous optical and patch-clamp measurements from adjacent points. These calibrations were conducted in voltage-clamp mode under conditions that favor good space clamp and accurate voltage control. Data demonstrating the resolution, linearity and accuracy of this technique will be presented. Representative ratiometric recordings of action potentials and synaptic potentials from the dendrites of cultured hippocampal neurons will be used to illustrate the usefulness of this approach.

M-PM-E9

ACOUSTO-OPTIC TUNABLE FILTERS FOR HIGH RESOLUTION LIGHT MICROSCOPY

E.S. Wachman, W. Niu, R.D. Shonat, A.P. Koretscky, and D.L. Farkas
Center for Light Microscope Imaging and Biotechnology,
Carnegie-Mellon University, Pittsburgh, PA 15213

We present recent improvements and applications of an acousto-optic microscope equipped with acousto-optic tunable filters (AOTFs) for both excitation and imaging. We have previously described [1] an AOTF imaging crystal enabling 0.35 μm resolution using high magnification optics and appropriate image processing. Here, we describe: 1) the use of an external dispersing prism to compensate directly for AOTF blur without the need for post-processing, resulting in negligible image distortion even at more modest magnifications; and 2) use of a multiline laser light excitation and oblique illumination to substantially improve the signal to background ratio, allowing high-resolution multicolor fluorescence images to be acquired of even weakly fluorescent samples.

The speed and spectral versatility of the acousto-optic microscope have numerous exciting biological applications. Here, we present some preliminary results demonstrating these capabilities including: 1) ratio image pairs captured in under 5 milliseconds; and 2) *in-vivo* phosphorescence lifetime images to measure oxygen tensions in mouse vasculature.

[1] Wachman, E.S., Niu, W., Farkas, D.L., "Imaging acousto-optic tunable filter with 0.35-micrometer spatial resolution," Applied Optics 35 (25), 5220 (1996).

ION MOTIVE ATPases I

M-PM-F1

A SINGLE MUTATION ^{885}D→R IN THE M7/M8 EXTRACELLULAR LOOP OF THE A SUBUNIT OF THE SODIUM PUMP ALTERS NA^+ BUT NOT K^+ RECOGNITION BY THE ENZYME. ((H. Schneider and **G. Scheiner-Bobis**)) Inst. f. Biochem. and Endocrinol., JLU, Giessen, Germany

Mutations were introduced in the motif ^{884}DDRW^{887} from an extracellular peptide of the sodium pump α subunit localized between M7 and M8 membrane spans because a homologous sequence ^{399}QDYW^{402} within the P-loops of Na^+ channels was shown earlier to be important for ion gating. Mutant sodium pumps were expressed in yeast and subsequently investigated for their behavior towards ouabain, Na^+, K^+ and ATP. Native enzyme and the ^{884}D→R or ^{885}D→R mutants all bind ouabain with high affinity in the presence of phosphate and Mg^{2+}. The K_D values determined from Scatchard analysis are 5.4, 15.8 and 29.9 nM, respectively. This ouabain binding is reduced in the presence of K^+ in a similar way for both native or mutant sodium pumps with $K_{0.5}$ values for K^+ ranging from 1.4-3.7 mM. Ouabain binding in the presence of 100 μM ATP is promoted by Na^+ with $K_{0.5}$=1.6 mM for the native and $K_{0.5}$=8.9 mM for the ^{884}D→R mutant. The relative affinities $K_{0.5}$ of the two enzymes for ATP are 0.65 μM and 0.94 μM, respectively. Ouabain binding as a function of Na^+ concentration cannot be detected with the ^{885}D→R mutant of the sodium pump even at ATP concentrations of 5 mM. These results suggest a cytosolic localization of the M7/M8 loop and a close contact of this sequence with intracellular Na^+ and ATP binding sites. Since, however, an extracellular localization of this sequence has been demonstrated, an alternative possible explanation is that the M7/M8 loop might be invaginated within the plane of the plasma membrane and possibly interact with cytosolic Na^+ and ATP sites. Such a structure would resemble the P-loops of Na^+ channels that participate in conduction of Na^+ ions.

M-PM-F2

Na/K PUMP-MEDIATED CHARGE MOVEMENTS REPORTING DEOCCLUSION OF 3 Na^+ ((J. Wagg, M. Holmgren, **D.C. Gadsby**, F. Bezanilla, R.F. Rakowski and P. De Weer)) Marine Biological Laboratory, Woods Hole, MA 02543, USA.

Translocation of 3 Na^+ by the Na/K-pump is thought to involve a slow conformational change allowing electrogenic release of the 1st Na^+ to the external medium via a high-field access channel, and then electrogenic release of the remaining 2 Na^+ via a low-field access channel. The resulting transient currents were obtained in squid (*Loligo pealei*) giant axons, superfused and internally dialyzed (10 mM MgATP, 100 mM Na) with K^+- and Cl^--free solutions to prevent Na/K cycling, by subtracting currents (filtered at ≤100 kHz, digitized ≤2 MHz) elicited by voltage steps from 0 mV to -160 to +125 mV with 100 μM dihydrodigitoxigenin from those without it. Four components were distinguished, all requiring external Na^+: slow (τ ~1 ms), medium (τ ~100 μs), fast (τ ≤30 μs), and ultrafast (τ <3 μs). As the latter two closely matched the 2 phases of capacity current decay, we attribute them to ultrafast (unresolved) pump-mediated electrogenic events, rate-limited by the speed of stepping the membrane potential. These fast components had a very small effective valence (roughly 0.2), increased in size as external [Na] ($[Na]_o$) was raised from 25-100 mM, but became an increasing fraction of total charge as $[Na]_o$ was lowered, comprising the majority at 25 mM $[Na]_o$, and are thus attributed to release of the last Na^+ ions. The slow component was strongly voltage dependent (effective valence ~1.0), and was more prominent at higher $[Na]_o$. At 400 mM $[Na]_o$, after long (≥3 ms) steps to large negative potentials, the return to 0 mV elicited almost exclusively slow charge movement. The medium component appeared at intermediate $[Na]_o$ levels, had an effective valence <0.5, and at 50 mM $[Na]_o$ its amplitude following large negative voltage steps increased as their duration was prolonged, consistent with this component reporting transitions among conformations with 1 or 2 Na^+ bound. These results thus support the proposed sequential release of 3 Na^+. The absence of any steeply voltage dependent ultrafast component implies negligible steady-state population of the high-field access-channel conformation. This, together with the relatively weak apparent voltage dependence of the medium component, suggests that a further conformational change separates release of the 2nd and 3rd Na^+ ions. (Supported by HHMI, and NIH HL36783, GM30376, NS22979 and NS11223)

M-PM-F3

STRUCTURE-FUNCTION RELATIONSHIPS OF CATION BINDING AND E_1E_2 TRANSITIONS IN Na, K-ATPase.

Per Amstrup Pedersen, J.H. Rasmussen, and **P.L. Jorgensen**, Biomembrane Research Centre, August Krogh Institute, Copenhagen University, 2100 Copenhagen OE, Denmark.(Spon. by S.J.D. Karlish)

Lethal Na,K-ATPase mutations can be expressed in high yield in yeast cell membranes devoid of endogenous activity. Our system for expression of Na,K-ATPase in yeast allows targeting of αβ-units with lethal substitutions at the phosphorylation site, Asp^{369}, or at presumptive cation sites in transmembrane segments IV, V, and VI: Glu^{327}, Asp^{779}, Asp^{804}, Asp^{808}, to the cell surface at the same concentration of α-subunit and sites for [^{3}H]-ATP or [^{3}H]-ouabain binding as for wild type Na,K-ATPase. Mutations to the phosphorylated Asp^{369} show that this residue has important short range functions in modulating the affinity for ATP. It also has long range effects on the E_1-E_2 equilibrium, which are coupled to reorientation of cation sites and changes in affinity for ouabain. The cation site mutations are characterised with respect to Na-dependent phosphorylation and K-displacement of [^{3}H]-ATP binding. They are expressed in amounts sufficient for analysis of ^{86}Rb and ^{204}Tl occlusion. The analysis shows that Glu^{327}, Asp^{804}, and Asp^{808} contribute to coordination of Na^+ in the E_1P[3Na] or E_2P[2Na] phosphoforms. Alternatively Glu^{327}, Asp^{779}, Asp^{808} and in particular Asp^{804} contribute carboxylate oxygens to coordination of K^+ in the occlusion cavity of the E_2[2K] conformation.

Ref.: Pedersen, P.A., Rasmussen, J.H. and Jorgensen, P.L. (1996) J. Biol. Chem. 271: 2514-2522; (1996) Biochemistry, in press.

M-PM-F4

ANTIBODY PROBES FOR Na,K-ATPase TOPOLOGY AND FUNCTION. ((**K.J. Sweadner**, M.S. Feschenko, T. Pacholczyk, and E. Arystarkhova)) Neuroscience Center, Mass. General Hospital, Charlestown, MA 02129.

Monoclonal antibodies can be useful probes of structure and function when they bind to native enzyme and when their epitopes can be determined. Epitopes for several Na,K-ATPase α subunit antibodies were mapped by protein fragmentation and by molecular techniques, including expression of cloned cDNA fragments with λgt11, and screening a random peptide phage display library. (A) One antibody was mapped to the same site that is phosphorylated by protein kinase C; antibody binding was quantitatively prevented by addition of the phosphate group. (B) Another antibody was mapped by protein fragmentation and by λgt11 expression of cDNA fragments, but when a phage display peptide library was screened, a mimotope was discovered instead of the natural epitope. A mimotope is a peptide that is unrelated in sequence, but is nonetheless capable of mimicking the epitope by binding to the antibody. The validity of the mimotope was confirmed by its reactivity with the antibody when expressed in λgt11. (C) Two alternative models for the folding of the H5-H6 transmembrane hairpin of the α subunit can be tested with a third antibody. It was originally mapped to a segment which is usually predicted to be intracellular. Because binding is actually extracellular, its epitope is being reinvestigated by molecular techniques. A cDNA fragment encompassing the H5-H6 and H7-H8 hairpins bound the antibody after expression in λgt11, validating the general location of the epitope. Mapping with smaller fragments is now planned. Supported by HL 36271.

M-PM-F5

LYS480 AND LYS501 OF THE α-SUBUNIT OF NA,K-ATPASE HAVE DIFFERENT MICROENVIRONMENTS. ((Sylvia Daoud, Svetlana Lutsenko and **Jack H. Kaplan**)) Department of Biochemistry and Molecular Biology, OHSU, Portland, OR 97201.

Lys501 in the ATP-binding domain of the Na,K-ATPase was shown to have a unique reactivity towards FITC and other aromatic isothiocyanates and it was preferentially labeled when treated with these reagents. Chemical modification of Na,K-ATPase with a positively charged analog of FITC (TRITC) results in the labeling of the α-subunit of the Na pump, however, surprisingly, the target of modification in this case is exclusively Lys480. TRITC-labeled peptide was identified by N-terminal amino-acid sequencing of the fluorescently labeled fragment, obtained after cyanogen bromide cleavage of the α-subunit of Na-pump. Unlike modification with FITC, NIPI or SITS labeling of Na,K-ATPase with TRITC is ligand-independent. Experiments on double labeling of the Na,K-ATPase with FITC and TRITC showed that preincubation of Na-pump with FITC did not prevent incorporation of TRITC, suggesting that these two reagents do not share the same binding pocket and probably both Lys480 and Lys501 are exposed at the surface of the α-subunit. Our data also indicate that the microenvironments of Lys480 and Lys501 differ significantly inspite of the close location of these residues in the primary sequence of the α-subunit. Supported by NIH R01 HL30315 and R01 GM39500 to JHK.

M-PM-F6

KINETIC INVESTIGATIONS OF CONFORMATIONAL CHANGES OF THE NA^+, K^+-ATPASE. ((D.J. Kane, K. Fendler, E. Grell, E. Bamberg, K. Taniguchi, J.P. Froehlich and **R. J. Clarke**)) Max-Planck-Institute for Biophysics, Frankfurt am Main, Germany; Hokkaido University, Sapporo, Japan; NIA, NIH, Baltimore, MD 21204, USA.

Widely varying rate constants, between 25 and 200 s^{-1}, have been reported for the rate-determining step of the Na^+ translocation sequence of the Na^+, K^+-ATPase cycle under similar experimental conditions using different experimental methods and diffierent probes. In order to clarify this situation, we have investigated the kinetics of the Na^+-related partial reactions of the pig kidney enzyme via electrical bilayer measurements after the photochemical release of ATP and via fluorescence stopped-flow mixing using the probes RH 421 and BIPM. Results obtained from all of these methods were consistent with a rate constant of about 200 s^{-1} at pH 7.5 and 24°C. The fluoresence signals were pH-dependent, decreasing in rate from 200 s^{-1} at pH 7.5 to around 80 s^{-1} at pH 6.2. It was found that concentrations of the probe RH 421 in the micromolar range inhibit the Na^+-related partial reactions of the enzyme. Previously reported lower values of the rate constant can be attributed to 1) underestimation of the dissociation constant of ATP for its high affinity binding site, 2) neglect of the effects of caged ATP, and 3) the use of inhibiting concentrations of RH 421. The ATP concentration dependence of the observed rate constant yielded an ATP dissociation constant of 10 μM. All of the results are consistent with the assumption of two major enzyme conformations inherent in the Albers-Post model of the Na^+, K^+-ATPase mechanism.

M-PM-F7

EXPRESSION OF NA/K-ATPASE ALPHA SUBUNIT ISOFORMS DURING NEURONAL DIFFERENTIATION AND MATURATION. ((Y. Choi*, L.C. Williamson^, E.A. Neale^,, T.D. Copeland#, M. Takahashi@, **M.W. McEnery***)) *Dept. of Physiology and Biophysics, Case Western Reserve Univ. Sch. of Med., Cleveland, OH 44106, ^Lab. Dev. Neurobiol., NICHD, NIH, #ABL-Basic Research Program, NCI-Frederick Cancer Research and Development Center, Frederick, MD 21702, and @Mitsubishi-Kasei Institute, Tokyo, Japan.

A monoclonal antibody (mAb 9A7) identifies all three isoforms of Na/K-ATPase alpha subunit by western blotting, immunohistochemical localization and immunoaffinity purification. As mAb 9A7 reacts with an epitope conserved in all three isoforms, it is a valuable reagent to investigate and compare the relative level of expression of the alpha1, alpha2 and alpha3 isoforms in a given tissue. The primary focus of these experiments is the temporal pattern of expression of Na/K-ATPase alpha subunit isoforms in developing rat brain, differentiating human neuroblastoma cell lines (IMR32 cells), and primary spinal cord neurons obtained from embryonic mice. The results of these experiments using mAb 9A7 in conjunction with characterized antibodies specific for the three alpha subunit isoforms, indicate tissue-dependent differences in the alpha subunit isoforms expressed throughout *in vitro* differentiation. Specifically, while the alpha3 isoform is expressed in each of these neuronal tissues, the presence of a second alpha isoform appears to be a hallmark of particular tissue. These results are significant as they establish a framework to understand the normal expression pattern of Na/K-ATPase in primary spinal cord neurons in culture and permit us in future studies to determine if perturbations in Na/K-ATPase expression occurs in response to agents which inhibit or enhance the process of spinal cord maturation.

M-PM-F8

HYPOTONIC SWELLING ALTERS THE VOLTAGE-DEPENDENCE OF THE NA^+-K^+ PUMP IN CARDIAC MYOCYTES.((N.L.Bewick, H. H. Rasmussen and D. W. Whalley))Cardiology Department, Royal North Shore Hospital, St Leonards, NSW, Australia 2065. (Spon. by D. Whalley).

The cardiac Na^+-K^+ pump is stimulated by cell swelling during exposure to hypotonic solutions. Since cell swelling is known to alter the voltage-dependence of stretch-sensitive ion channels we examined the effect of hypotonicity on the voltage-dependence of the pump. Myocytes were voltage-clamped at -40 mV with patch-pipettes containing 10 mM Na^+. Swelling was induced by superfusion with hypotonic Tyrode's solution (240 mosM/L) containing 105 mM Na^+. Isotonic solutions (300 mosM/L) were identical to the hypotonic superfusates apart from the addition of 70 mM sucrose. We recorded steady-state currents elicited by test potentials (V_m) from -100 to + 60 mV. Na^+-K^+ pump current (I_p) was defined as the ouabain (100 μM) induced shift in holding current. I_p was recorded from myocytes superfused with isotonic solution (n=6,○) and hypotonic solution (n=6,● see fig). The data at each V_m is normalised relative to I_p recorded at V_m of 0 mV. The slope of the I_p-V_m relationship was significantly less steep for myocytes exposed to hypotonic solutions. Stimulation of the insulin receptor tyrosine kinase (TK) reduces the I_p-V_m relationship of the pump. We examined the effect of tyrphostin A25 (tyr A25, 100 μM), a specific inhibitor of TK. Tyr A25 eliminated the effect of hypotonicity on the slope of the I_p-V_m relationship. We conclude that the I_p-V_m relationship is regulated via a TK dependent mechanism in osmotically swollen cells.

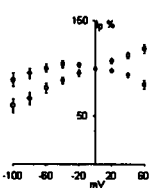

K CHANNELS: GATING

M-Pos1

CONTRIBUTIONS OF L1 AND L2 HEPTAD LEUCINES TO STABILIZATION OF THE OPEN STATE IN *SHAKER B* K^+ CHANNELS. ((**M. Hermosura**, M. Andres, J. Lu, J. Starkus and M. Rayner)) Bekesy Lab of Neurobiology, PBRC, University of Hawaii, Honolulu, HI.

Using thermodynamic analysis of a pseudo first-order deactivation-reactivation reaction, we have previously shown that mutations of the L1 heptad leucine in the S4 segment reduce open state stability in inactivation-removed *Shaker B* K+ channels (Andres et al.,1996 *Biophys.J.*, Abstr.; Rayner et al.,1996 *Biophys.J.*,Abstr).

We now extend this study to include effects at the L2 site and double mutations at both L1-L2 sites. Specifically, we have looked at effects of L to F and L to V substitutions at each site (ie., F1, V1, F2, and V2), plus that of the combined F1V2 double mutant. Observed ΔΔG shifts relative to wild-type were: **+1.3** for F1, **+2.0** for V1, **+1.8** for F2,**+2.3** for V2, and **+3.5** for F1V2. Since the observed F1V2 shift is not significantly different from the calculated total for F1 and V2 (**+3.6**) we conclude that hydrophobic interactions due to L1 and L2 act in a parallel and additive manner in stabilizing the open state. Moreover, effects from each site appear quantitatively similar as seen from ΔΔG shifts of **+2.0** for V1, **+2.3** for V2 and **+1.3** for F1 and **+1.8** for F2, suggesting similar interaction mechanisms at these sites.

Supported by NIH grant RO1 NS21151 and by awards from the American Heart Association (Hawaii Affiliate).

M-Pos2

ANOMALOUS CONDUCTION IN *SHAKER* B K^+ CHANNELS: CONDUCTION IN "NON-CONDUCTING" MUTANTS WITH MODIFIED S4 SEGMENTS. ((**M. Henteleff**, H. Bao, A. Hakeem, J. Starkus and M. Rayner)) Bekesy Lab. of Neurobiology, PBRC, Univ of Hawaii, Honolulu, HI.

In N-terminus deleted *Shaker* B channels, the W434F pore domain mutation typically prevents permeation by potassium ions. We describe here S4 mutations which modify the action of W434F, such that K^+ currents remain although channel gating becomes voltage-insensitive.

In a series of S4 mutants with multiple charge-neutralizations, we find voltage-sensitive gating with parameters similar to channels with unmodified S4 segments. In mutants from this series in which either charges 1 and 2 or charges 1, 4 and 7 were neutralized, addition of W434F resulted in maintained K^+ currents in which conductance is unaffected by changes in membrane potential between -160 and +100 mV. However, back mutation from glutamine to arginine at the 1st charge site restores both normal voltage-sensitive gating and the expected "non-conducting" behavior of the W434F mutation.

We conclude that the W434 residue normally interacts both with the permeation pathway and with charges towards the N-terminus end of the S4 segment. The W434 residue may thus be a significant component of the mechanism by which channels are "gated" into conducting or non-conducting states by S4 movement.

Supported by NIH grant RO1 NS21151 and by awards from the American Heart Association (Hawaii Affiliate).